Budget of nitrous acid (HONO) at an urban site in the fall season of Guangzhou, China

Yihang Yu[1,2], Peng Cheng[1,2,5,*], Huirong Li[1,2], Wenda Yang[1,2], Baobin Han[1,2], Wei Song[3], Weiwei Hu[3], Xinming Wang[3], Bin Yuan[4,5], Min Shao[4,5], Zhijiong Huang[4], Zhen Li[4], Junyu Zheng[4,5], Haichao Wang[6] and Xiaofang Yu[1,2]

[1]Institute of Mass Spectrometry and Atmospheric Environment, Jinan University, Guangzhou 510632, China
[2]Guangdong Provincial Engineering Research Center for Online Source Apportionment System of Air Pollution, Guangzhou 510632, China
[3]State Key Laboratory of Organic Geochemistry, Guangzhou Institute of Geochemistry, Chinese Academy of Sciences, Guangzhou 510640, China
[4]Institute for Environmental and Climate Research, Jinan University, Guangzhou 511443, China
[5]Guangdong-Hongkong-Macau Joint Laboratory of Collaborative Innovation for Environmental Quality, Guangzhou 511443, China
[6]School of Atmospheric Sciences, Sun Yat-Sen University, Zhuhai, China

*Correspondence to: Peng Cheng (chengp@jnu.edu.cn)

Abstract. High concentrations of nitrous acid (HONO) have been observed in the Pearl River Delta (PRD) region of China in recent years, contributing to elevated atmospheric oxidation capacity by producing OH through HONO photolysis. We have investigated budget of HONO at an urban site in Guangzhou from 27 September to 9 November 2018 using data from a comprehensive atmospheric observation campaign. During this period, HONO was measured from 0.02 to 4.43 ppbv with an average of 0.74 ± 0.70 ppbv. Emission ratios (HONO/NOx) of $0.9 \pm 0.4\%$ were derived from 11 fresh plumes. The primary emission rate of HONO at night was calculated to be between 0.04 ± 0.02 ppbv h^{-1} and 0.30 ± 0.15 ppbv h^{-1} based on a high-resolution NOx emission inventory. Heterogeneous conversion of NO_2 on ground surface (0.27 ± 0.13 ppbv h^{-1}), primary emission from vehicle exhaust (between 0.04 ± 0.02 ppbv h^{-1} and 0.30 ± 0.15 ppbv h^{-1} with a middle value of 0.16 ± 0.07 ppbv h^{-1}) and the homogeneous reaction of NO + OH (0.14 ± 0.30 ppbv h^{-1}) were found to be the three largest sources of HONO at night. Heterogeneous NO_2 conversion on the aerosol surfaces (0.03 ± 0.02 ppbv h^{-1}) and soil emission (0.019 ± 0.009 ppbv h^{-1}) were two other minor sources. Correlation analysis shows that NH_3 and relative humidity (RH) may have participated in the heterogeneous transformation from NO_2 to HONO at night. Dry deposition (0.41 ± 0.31 ppbv h^{-1}) was the largest removal process of HONO at night, followed by dilution (0.18 ± 0.16 ppbv h^{-1}), while HONO loss on aerosol surfaces was much slower (0.008 ± 0.006 ppbv h^{-1}). In the daytime, the average primary emission P_{emis} was 0.12 ± 0.02 ppbv h^{-1}, and the homogeneous reaction P_{OH+NO} was 0.79 ± 0.61 ppbv h^{-1}, larger than the unknown source $P_{Unknown}$ (0.65 ± 0.46 ppbv h^{-1}). Similar to previous studies, $P_{Unknown}$ appeared to be related to the photo-enhanced conversion of NO_2.

Our results show that primary emissions and reaction of NO + OH can significantly affect HONO at a site with intensive emissions, both during daytime and nighttime. The impact of uncertain parameter values assumed in the calculation of HONO sources can have strong impact on the relative importance of HONO sources at night, and could be reduced by

35 improving knowledge on key parameters such as the NO_2 uptake coefficient. The uncertainty with estimating direct emission can be reduced by using emission data with higher resolution and quality. Our study highlights the importance of better constraining both conventional and novel HONO sources by reducing uncertainties in their key parameters in advancing our knowledge on this important source of atmospheric OH.

40 Keywords: HONO; Budget analysis; Heterogeneous reaction; Uncertainty

1 Introduction

Nitrous acid (HONO) is an important primary source of hydroxyl radical (OH) through photolysis (Reaction R1), contributing up to 33–92% OH at rural and urban sites (Kleffmann et al., 2005; Michoud et al., 2012; Tan et al., 2017; Xue et al., 2020; Hendrick et al., 2014). OH is the principle atmospheric oxidant that is responsible for oxidizing and removing

45 most natural and anthropogenic trace gases. OH initiates the oxidation of the volatile organic compounds (VOC) to produce hydroperoxyl radicals (HO_2) and organic peroxy radicals (RO_2), which further lead to the formation of ground-level ozone (O_3) in the presence of nitrogen oxides (NOx = NO + NO_2) (Xue et al., 2016; Finlayson-Pitts and Pitts, 2000; Hofzumahaus et al., 2009; Lelieveld et al., 2016; Tan et al., 2018), as well as secondary organic aerosols (SOA). However, the detailed formation mechanisms of HONO are still not well understood and the observed HONO concentrations cannot be completely

50 explained by current knowledge (Sörgel et al., 2011a; Kleffmann et al., 2005; ~~Sarwar et al., 2008;~~ Liu et al., 2019a; Lee et al., 2016; Liu et al., 2020b; Pusede et al., 2015).

$$HONO + hv \rightarrow OH + NO \ (300 \text{ nm} < \lambda < 405 \text{ nm}) \tag{R1}$$

55 So far numerous HONO sources have been found, and they can be categoried as direct emissions, homogeneous reactions and heterogeneous reactions. Fossil fuel combustion is the most important direct emission source of HONO (Kurtenbach et al., 2001; Kirchstetter et al., 1996; Rappenglück et al., 2013; Kramer et al., 2020; Xu et al., 2015; Trinh et al., 2017). In general, the emission ratios of HONO/NOx obtained from fresh air masses ~~and~~ mixed with vehicle exhaust (0.03%–1.7%) (Kurtenbach et al., 2001; Kirchstetter et al., 1996; Rappenglück et al., 2013; Trinh et al., 2017; Liu et al., 2017; Pitts et al.,

60 1984; Nakashima and Kajii, 2017) are much smaller than the ratios of HONO/NOx observed in the low boundery layer (2.3%–9%) (Yang et al., 2014; Zhou et al., 2002a; Hao et al., 2020; Gu et al., 2021; Li et al., 2018a; Yu et al., 2009; Acker et al., 2006; Kleffmann et al., 2003; VandenBoer et al., 2013; Vogel et al., 2003), reflecting substantial secondary formation of HONO away from direct emissions. Recent studies found that soil emission might be another major direct emission source of HONO (Su et al., 2011; Oswald et al., 2013; Weber et al., 2015; Wu et al., 2019; ~~Porada et al., 2019~~; Wang et al., 2021b),

65 although the confirmation of its atmospheric significance requires further comparisons between laboratory and field

measurements. It should be noted that direct emissions may surpass secondary sources at sampling sites with heavy emission impacts (Liu et al., 2019a; Tong et al., 2015; Zhang et al., 2019; Tong et al., 2016; Meusel et al., 2016).

Homogeneous gas-phase reaction between NO and OH (R2) is the most well known secondary source of HONO (Perner and Platt, 1979). HONO concentrations measured in the atmosphere cannot be explained by direct emission and this reaction alone, especially during daytime (Kleffmann et al., 2005; Lee et al., 2016) when a large source of HONO is necessary to sustain the measured level of HONO against fast photolysis. Some ~~Numerous new~~ homogeneous HONO formation mechanisms have been proposed so far to explain the gap between observed and predicted HONO, including HONO formation by photolysis of o-nitrophenol (Bejan et al., 2006; Yang et al., 2021a), ~~homogeneous nucleation of NH₃, NO₂ and H₂O (Zhang and Tao, 2010), and~~ the homogeneous reaction between ~~water vapor (H₂O) and electronically excited NO₂ (λ > 420 nm) followed by~~ and the reaction of NO_2 with $HO_2 \cdot H_2O$ (~~Li et al., 2008;~~ Li et al., 2014b). But they ~~These gas phase reactions~~ have yet to be confirmed to occur in the atmosphere, and are unlikely to be the main HONO source.

$$NO + OH \rightarrow HONO \qquad\qquad (R2)$$
$$2NO_2 + H_2O \rightarrow HONO + HNO_3 (surface) \qquad\qquad (R3)$$
$$NO_2 + red_{ads} \rightarrow HONO + ox_{ads} \qquad\qquad (R4)$$

Heterogeneous reactions of NO_2 on various surfaces have drawn substantial interest due to the observed correlation between HONO and NO_2 during many field observations. Vertical gradient observations ~~appear to~~ suggest that HONO is more likely produced from the ground surface (Wong et al., 2012; Kleffmann et al., 2003; Stutz et al., 2002; VandenBoer et al., 2013; Wong et al., 2011; Villena et al., 2011), while some observations found a good correlation between HONO and aerosol surface area (Reisinger, 2000; Su et al., 2008a; Jia et al., 2020; Zheng et al., 2020; Liu et al., 2014), which can be related to the concentration and composition of particulate matter (Cui et al., 2018; Liu et al., 2014; Colussi et al., 2013; Yabushita et al., 2009; Kinugawa et al., 2011). Both laboratory studies and field observations have found that hydrolysis of NO_2 on wet surfaces can produce HONO (R3), and the uptake coefficient of NO_2 (γ) can vary by several orders of magnitude (Finlayson-Pitts et al., 2003; Stutz et al., 2004; Acker et al., 2004). HONO can also be generated by NO_2 reduction on various ~~reductive~~ surfaces (soot, semivolatile organic compounds, humic acid, etc.) at a much faster rate than NO_2 hydrolysis, but the surfaces could be inactivated in a short period of time (Ammann et al., 1998; Han et al., 2017a; Han et al., 2017b; Gerecke et al., 1998; Monge et al., 2010; Gutzwiller et al., 2002; Wall and Harris, 2017; Stemmler et al., 2006; Aubin and Abbatt, 2007). However, irradiation could enhance the reaction and maintain the activity of the surfaces, making it possible to play an important role in HONO formation during daytime. Both laboratory and field studies found that photolysis of adsorbed HNO_3 and particulate nitrate (NO_3^-) could produce HONO (Ye et al., 2016; Ye et al., 2017; Zhou et al., 2003; Zhou et al., 2002b; Zhou et al., 2011), which might be an important HONO source, at least in remote areas and polar regions. Evidence

of other new pathways and mechanisms has also been found and their atmospheric relevance discussed (Ge et al., 2019; Wang et al., 2016; Xu et al., 2019; Li et al., 2018b; Xia et al., 2021; Zhao et al., 2021; Gen et al., 2021).

The Pearl River Delta (PRD) region is one of the biggest city clusters in the world with dense population and large anthropogenic emissions. Rapid economic development and urbanization have led to severe air pollution in this region, which has been characterized by atmospheric "compound pollution" with concurrently high fine particulate matter ($PM_{2.5}$) and ozone (O_3) (Tang, 2004; Chan and Yao, 2008; Yue et al., 2010; Wang et al., 2017b; Xue et al., 2014; Zheng et al., 2010). Over recent years, O_3 has been increasing along with reduced $PM_{2.5}$ in the region (Li et al., 2014a; Liao et al., 2020; Wang et al., 2009; Zhong et al., 2013; Lu et al., 2018), and has become the dominant factor of the air quality index exceeding the national standard (Feng et al., 2019), indicating the enhancement of atmospheric oxidation capacity. So far, two comprehensive atmospheric observations have been conducted in the PRD region, focusing on the balance and dynamics of OH sources and sinks (Hofzumahaus et al., 2009; Tan et al., 2019). Substantial amount of HONO was suggested to be a major source of the OH–HO_2–RO_2 radical system in these two campaigns (Lu et al., 2012; Tan et al., 2019) as well as in other previous campaigns (Hu et al., 2002; Su et al., 2008b; Su et al., 2008a; Qin et al., 2009; Li et al., 2012; Shao et al., 2004).

In this work, we performed continuous measurements of HONO, along with trace gases, photolysis frequencies and meteorological conditions at an urban site in Guangzhou from 27 September to 9 November 2018, as part of the field campaign "Particles, Radicals, Intermediates from oxiDation of primary Emissions in Greater Bay Area" (PRIDE-GBA2018). Benefiting from numerous prior field observational studies in the PRD region, our study stands in a strong position to ensure high quality of data acquisition and analysis of HONO, along with a full suite of other chemical species, providing a unique and valuable opportunity to refine our knowledge of HONO sources and sinks, as well as the role of HONO in the photochemistry of O_3 and OH in such a region with extensive air pollution as well as rigorous emission control over recent years.

Departing from the valuable knowledge and experiences gained from numerous previous HONO studies in the PRD region and around the world, we aim to draw useful and unique insights from a detailed analysis of our dataset in the context of a comprehensive review of previous data and findings, with special attention paid to reducing and/or characterizing the uncertainties in parameterizations and their implications on the relative importance of various HONO sources and sinks. Specifically, (1) a high resolution (3 km × 3 km) NOx emission inventory for the Guangzhou city (Huang et al., 2021) was used to estimate the primary emission rates of NOx and HONO, which would reduce the uncertainty of HONO primary emission rate; (2) a wide range of possible parameter values have been evaluated for each source to quantify their strengths and rank their importance; (3) uncertainties associated with each source and other possible factors are discussed in detail.

2 Experiment

2.1 Observation site

The sampling site (23.14° N, 113.36° E) is located in the Guangzhou Institute of Geochemistry Chinese Academy of Sciences (GIGCAS). The instruments were deployed in the cabin on the rooftop of a seven-story building (~ 40 m above the ground). The site is surrounded by residential communities and schools, with no industrial manufacturers or power plants around, representing a typical urban environment in the PRD region. The south China Expressway and Guangyuan Expressway, both with heavy traffic loading, are located at west and south of the site, with distances of about 300 m. As a result, the site often experienced local emissions from traffic. The location and surroundings of the site are shown in Fig. S1.

2.2 Measurements

HONO was measured by a custom-built LOPAP (LOng Path Absorption Photometer) (Heland et al., 2001; Kleffmann et al., 2006). More information about our custom-built LOPAP (including principle, quality assurance/quality control, instrument parameters and intercomparison) are introduced in supplement information.

In addition to HONO, ~~ambient VOCs were measured using a TH 300B On Line VOCs Monitoring System involving detection technology of ultralow temperature preconcentration coupled with gas chromatography mass spectrometry (GC/MS) with the time resolution of 1 h.~~ NOx (NO + NO$_2$) was measured by a nitrogen oxides analyzer (Thermo Scientific, Model 42i), which used a NO-NOx chemiluminescence detector equipped with a molybdenum-based converter with the time resolution and detection limit of 1 min and ~~1~~ 0.4 ppbv respectively. It should be noted that the molybdenum oxide (MoO) converters may also convert some NOz (= NOy - NOx) (e.g., HONO, peroxyacetyl nitrate (PAN), HNO$_3$, and so on.) species to NO and hence could overestimate the ambient NO$_2$ concentrations. The degree of overestimation depends on both air mass age and the composition of NOy. At our site that was greatly affected by fresh emissions, the relative interferences of NOz to NO$_2$ have been estimated to be around 10% (see supplement information), which is closed to the results of Xu et al. (2013) and negligible for our discussion of HONO budget. O$_3$ was measured by an O$_3$ analyzer (Thermo Scientific, Model 49i) via ultraviolet absorption method with the time resolution and detection limit of 1 min and 1 ppbv respectively. SO$_2$ was measured by SO$_2$ analyzer (Thermo Scientific, Model 43i) via pulsed fluorescence method with the time resolution and detection limit of 1 min and 0.5~~1~~ ppbv respectively. CO was measured by a CO analyzer (Thermo Scientific, Model 48i) with the time resolution and detection limit of 1 min and 0.04~~0.1~~ ppmv respectively. NH$_3$ was measured by laser absorption spectroscopy (PICARRO, G2508) with the precision of < 3 ppbv at 1 min~~time resolution and detection limit of 1 min and 1 ppbv respectively~~. Gaseous HNO$_3$ was detected by a Time-Of-Flight Chemical Ionization Mass Spectrometer (Aerodyne Research Inc., TOF-CIMS) with a time resolution of 1 min. And particulate nitrate (NO$_3^-$) was measured by Time-Of-Flight Aerosol ~~Accelerator~~ Mass Spectrometry (Aerodyne Research Inc., TOF-AMS) with a time resolution of 1 min. PM$_{2.5}$ was measured by a Beta Attenuation Monitor (MET One Instruments Inc., BAM-1020) with the time resolution and detection

165 limit of 1 h and 4.0 µg m^{-3} respectively. The meteorological data, including temperature (T), relative humidity (RH) and wind speed and direction (WS, WD) were recorded by Vantage Pro2 Weather Station (Davis Instruments Inc., Vantage Pro2) with the time resolution of 1 min. Photolysis frequencies including J(HONO), J(NO$_2$), ~~J(H$_2$O$_2$)~~ and J(O^{1}D) were measured by a spectrometer~~filter radiometry~~ (Focused Photonics Inc., PFS-100) with a time resolution of 1 min.

3 Results and discussion

170 **3.1 Data overview**

The time series of meteorological parameters and pollutants during the campaign are shown in Fig. 1. The HONO concentrations ranged from 0.02 to 4.43 ppbv with an average of 0.74 ± 0.70 ppbv. Table 1 summarizes the HONO observations reported in PRD region since 2002. HONO appears to have shown a decreasing trend in Guangzhou, as improvement of air quality in Guangzhou was witnessed during the past decade. Spikes of NO occurred frequently, even up 175 to 134.8 ppbv, as a result of traffic emissions from two major roads near the site. The concentrations of NO$_2$, SO$_2$, NH$_3$ and PM$_{2.5}$ ranged from 5.4–102.0 ppbv, 0–6.3 ppbv, 2.8–7.8 ppbv and 4–109 µg m^{-3} respectively with the average values of 50.8 ± 17.2 ppbv, 1.9 ± 1.2 ppbv, 6.3 ± 2.7 ppbv, and 36 ± 16 µg m^{-3} respectively. The O$_3$ concentrations ranged from 0.3–149.8 ppbv with an average peak concentration of 73.9 ± 28.4 ppbv. During the observation, the temperature ranged from 17 °C to 30 °C with an average of 24 ± 3 °C, and the relative humidity ranged from 28% to 97% with an average of 70 ± 17%. The 180 average wind speed was 6.8 ± 4.5 m s^{-1}, while the maximum wind speed was 22.7 m s^{-1}. There was a pollution period from 8th to 10th October with elevated PM$_{2.5}$ (60 ± 12 µg m^{-3}) and HONO (0.94 ± 0.58 ppbv). By contrast, from 29 October to 3 November, efficient ventilation driven by strong winds (> 11 m s^{-1}) led to low levels of most pollutants in this period, with average concentrations of PM$_{2.5}$ and HONO at 28 ± 11 µg m^{-3} and 0.56 ± 0.34 ppbv, respectively.
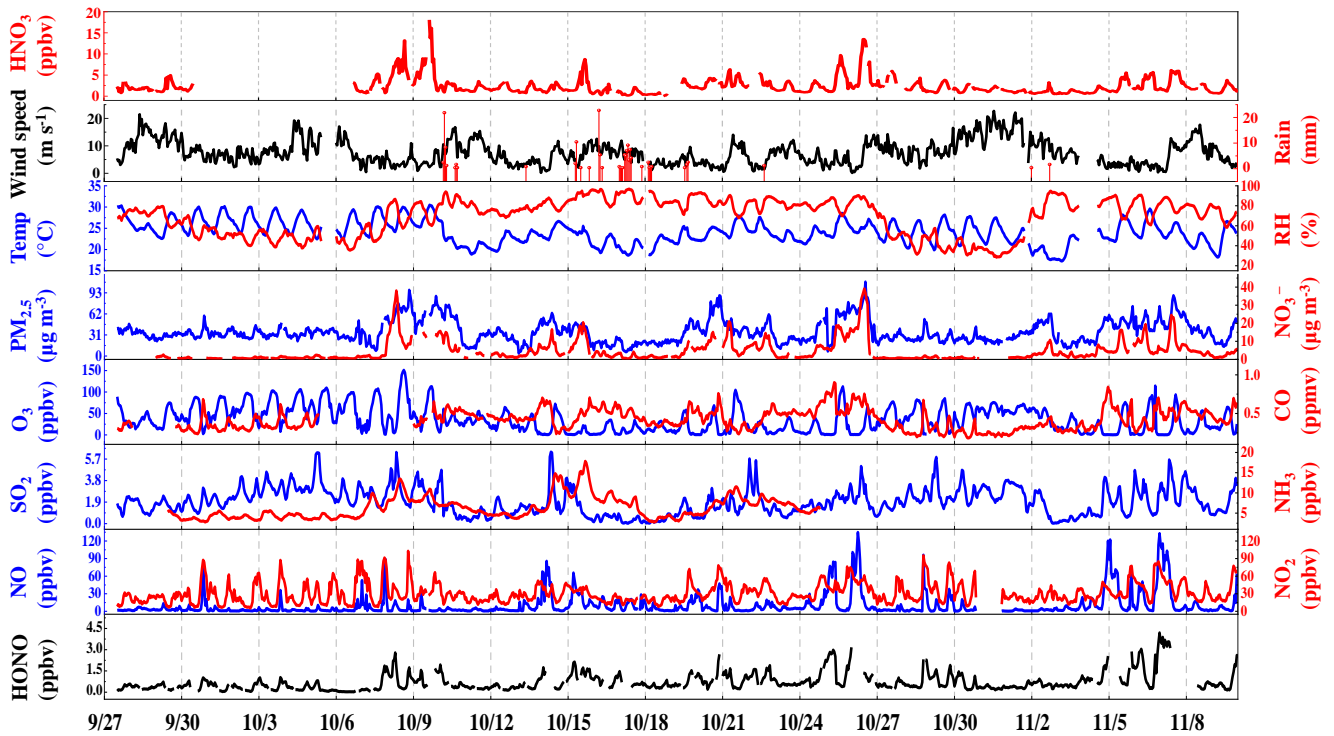
185

Figure 1. Temporal variations of meteorological and pollutants during the observation period.

Table 1. Overview of the ambient HONO, NO₂ and NOx measurement, as well as the ratios of HONO/NO₂ in the PRD region ordered chronologically. Data from Guangzhou are in italic.

Location	Date	HONO (ppbv)	HONO (ppbv)	HONO (ppbv)	NO₂ (ppbv)	NO₂ (ppbv)	NOx (ppbv)	NOx (ppbv)	HONO/NO₂	HONO/NO₂	Reference
			Night	Day	Night	Day	Night	Day	Night	Day	
Guangzhou (China)	*Jul 2002*	*1.89*	–	–	–	–	–	–	–	–	*1*
	Nov 2002	*1.52*	–	–	–	–	–	–	–	–	
Xinken (China)	*Oct–Nov 2004*	*1.20*	*1.30*	*0.80*	*34.8*	*30.0*	*37.8*	*40.0*	*0.037*	*0.027*	*2*
Back Garden (China)	*Jul 2006*	*0.93*	*0.95*	*0.24*	*16.5*	*4.5*	*20.9*	*5.5*	*0.057*	*0.053*	*3*
Guangzhou (China)	*Jul 2006*	*2.80*	*3.50*	*2.00*	*20.0*	*30.0*	–	–	*0.175*	*0.067*	*4*
Guangzhou (China)	*Oct 2015*	*1.64*	*2.25*	*0.90*	*40.5*	*27.3*	*57.9*	*39.8*	*0.060*	*0.030*	*5*
Guangzhou (China)	*Jul 2016*	*1.03*	*1.27*	*0.70*	*35.0*	*25.9*	*66.3*	*52.1*	*0.040*	*0.070*	*6*
Guangzhou (China)	*Sep–Nov 2018*	*0.74*	*0.91*	*0.44*	*36.9*	*23.3*	*47.7*	*30.1*	*0.026*	*0.022*	*–*
Jiangmen (China)	Oct–Nov 2008	0.60	–	0.48	–	–	–	9.1	–	–	7
	Aug 2011	0.66	0.66	0.70	21.8	18.1	29.3	29.3	0.031	0.042	
Hong Kong (China)	Nov 2011	0.93	0.95	0.89	27.2	29.0	37.2	40.6	0.034	0.030	8
	Feb 2012	0.91	0.88	0.92	22.2	25.8	37.8	48.3	0.036	0.035	
	May 2012	0.35	0.33	0.40	14.7	15.0	19.1	21.1	0.022	0.030	
Hong Kong (China)	Sep–Dec 2012	0.13	–	–	–	–	–	–	–	–	9
Heshan (China)	Oct 2013	1.57	–	–	–	–	–	–	–	–	10
Heshan (China)	Oct–Nov 2014	1.40	1.78	0.77	19.3	17.9	21.5	22.7	0.093	0.055	11
Hong Kong (China)	Mar–May 2015	3.30	2.86	3.91	–	–	–	–	–	–	12
Heshan (China)	Jan 2017	2.70	3.10	2.30	–	–	–	–	0.116	0.089	13

References:1: Hu et al. (2002); 2: Su et al. (2008a) and Su et al. (2008b); 3: Su (2008) and Li et al. (2012); 4: Qin et al. (2009); 5: Tian et al. (2018); 6: Yang et al. (2017a); 7: Yang (2014); 8: Xu et al. (2015); 9: Zha et al. (2014); 10: Yue et al. (2016); 11: Liu (2017); 12: Yun et al. (2017); 13: Yun (2018).

190

The time series of photolysis frequencies J(HONO), J(O^{1}D) and J(NO$_2$) in the whole observation period are shown in Fig. S3. The maximum values of J(HONO), J(O^{1}D) and J(NO$_2$) are 1.58×10^{-3} s^{-1}, 2.54×10^{-5} s^{-1} and 9.31×10^{-3} s^{-1}, respectively. These J values tracked a similar diurnal pattern, reaching a maximum at noon with high solar radiation and decreasing to zero at night.

The diurnal variations of HONO, NO$_2$, HONO/NO$_2$, and NO are shown in Fig. 2. A daytime trough and a night-time peak of HONO were observed, as typically seen at urban and rural sites (Lee et al., 2016; Xue et al., 2020; Villena et al., 2011; Yang et al., 2021b). The observed high HONO concentration around 0.5 ppbv at daytime implies strong HONO production to balance its rapid loss through photolysis. NO$_2$ showed a similar diurnal pattern. It is worth noting that the diurnal variation of NO was quite similar to that of HONO, implying the potential association between them. Additionally, the observed large amount of NO (10.8 ± 17.2 ppbv) at night indicated strong primary emission near the site. As an indicator of NO$_2$ to HONO conversion, the ratio of HONO/NO$_2$ rose at night and decreased after sunrise due to photolysis, ranging from 0.002 to 0.0910.2% to 9.1% with an average of 0.023 ± 0.0132.3 ± 1.3%, which is lower than most previous field observations in the PRD region (Li et al., 2012; Qin et al., 2009; Xu et al., 2015), and is typical for relatively fresh plumes (Febo et al., 1996; Lammel and Cape, 1996; Sörgel et al., 2011b; Stutz et al., 2004; Zhou et al., 2007; Su et al., 2008a).
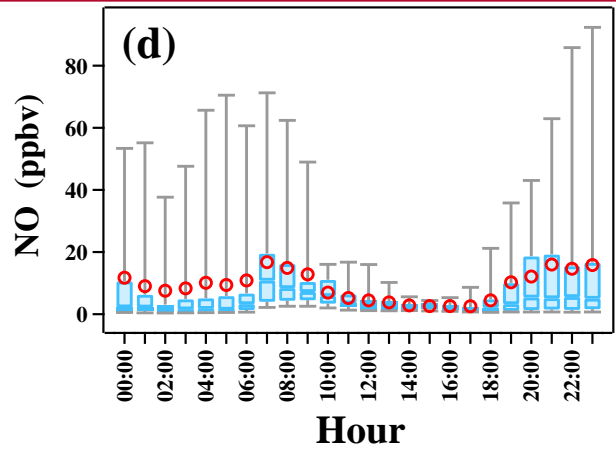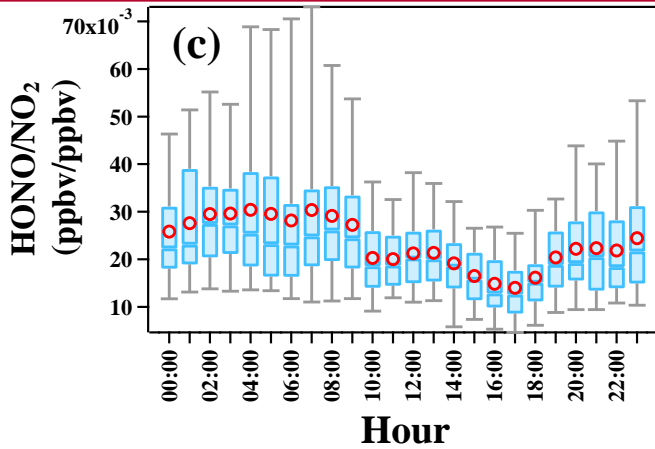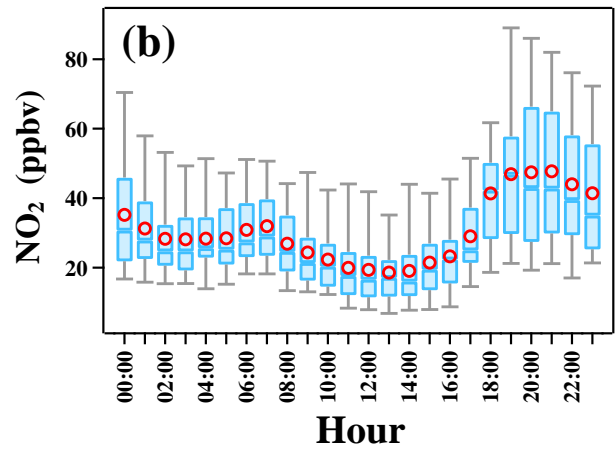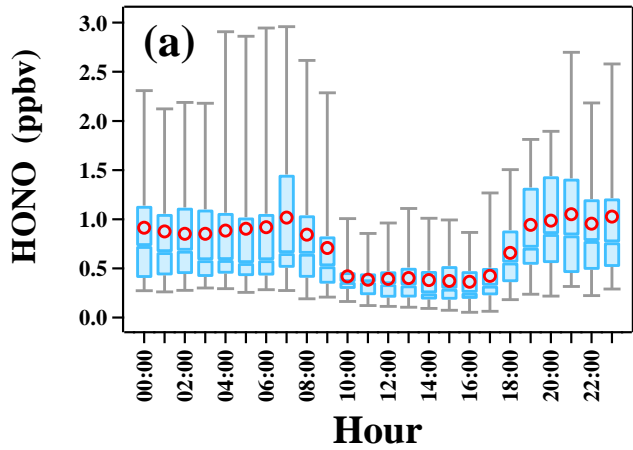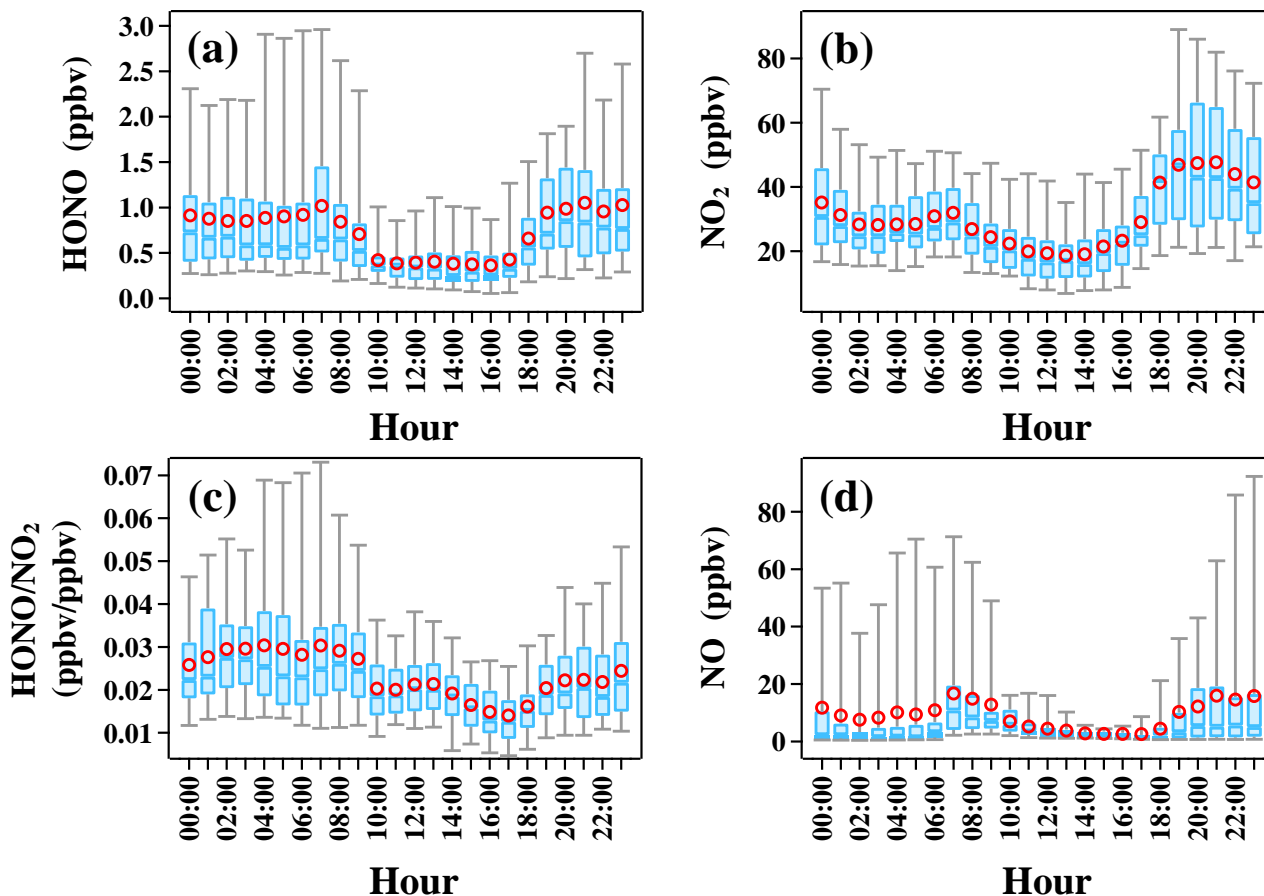
Figure 2. Diurnal profiles of (a) HONO, (b) NO₂, (c) HONO/NO₂~~NO~~ and (d) NO~~HONO/NO₂~~ during the observation period. The blue line in the box and red circle refer to the median and mean, respectively. Upper and lower boundaries of the box represent the 75th and the 25th percentiles; the whiskers above and below each box represent the 95th and 5th percentiles. ~~Boxes represent 25% to 75% of the data, and whiskers 95% of the data.~~ The box plots presented in this study is generated by an Igor Pro-based computer program, Histbox (Wu et al., 2018).

3.2 Nocturnal HONO sources and sinks

3.2.1 Direct emissions

As noted in Sect. 2.1, the site was expected to receive substantial direct emission of HONO from two major roads nearby. We obtained the emitted HONO/NOx ratios in fresh plumes defined with the following criteria (Xu et al., 2015): (a) NOx > 49.7 ppbv (highest 25% of NOx data);(b) NO/NOx > 0.8; (c) good correlation between NOx and HONO ($R^2 > 0.70$, $P < 0.05$); (d) short duration of plumes (< 2 h); (e) global radiation < 10 W m⁻² ($J(NO_2) < 0.25 \times 10^{-3}$ s⁻¹).

During the campaign, 11 fresh plumes were identified to satisfy all of the criteria ~~criteria (a)–(e)~~ (see Table S2). Two cases among them are shown in Fig. S4. The HONO/NOx ratios in these selected plumes varied from 0.1% to 1.5% with an average value of 0.9 ± 0.4%, which is comparable to the average value of 1.2% (Xu et al., 2015) and 1.0% (Yun et al., 2017) measured in Hong Kong ~~(Xu et al., 2015), 1.0% observed in Hong Kong (Yun et al., 2017)~~, 0.79% measured in Nanjing (Liu et al., 2019b) and 0.69% observed in Changzhou (Shi et al., 2020). It should be noted that the emission factor derived in this study was based on field observation and the screening criterion for fresh air mass was NO/NOx > 0.8, while the fresh air mass was characterized by NO/NOx > 0.9 in the tunnel experiments conducted by Kurtenbach et al. (2001), so the air masses we selected were still slightly aged and the emission factor derived in this study is slightly overestimated.

To quantify the primary emission rate of HONO, three methods have been used in previous studies (Liu et al., 2019b; Liu et al., 2020a; Meng et al., 2020). In method (1), the observed NOx concentration is ~~simply~~ assumed to represent the accumulation of emissions but ignore the sinks of NOx and HONO, as well as transport and convection. On this basis, $[HONO]_{emis}$ (the primary emission's contribution to HONO concentration) is estimated as the product of emission coefficient K and observed NOx concentration (Cui et al., 2018; Huang et al., 2017) (see Eq. (1)). Since it is difficult to determine the time of NOx emissions, method (1) can not exclude the NOx levels before emission begins. With this in mind, in method (2), primary emission rate P_{emis} is estimated as the product of emission coefficient K and $[\Delta NOx]/\Delta t$, where $[\Delta NOx]$ is the difference between observed NOx at two time points (Liu et al., 2019b; Zheng et al., 2020) (see Eq. (2)). Obviously, it can only be used when NOx is increasing. It should be noted that any loss of NOx and HONO can be a source of error for these two methods, especially during daytime. In method (3), primary emission rate P_{emis} is equal to the product of emission coefficient K and NOx*, the NOx emission from source emission inventory (Michoud et al., 2014; Su et al., 2008b) (see Eq. (3)). This method adheres to the definition of HONO emission rate, assuming that the primary sources are evenly mixed in a specific area. It is desirable to use emission inventory data with high spatial and temporal resolution to obtain an accurate estimate.

$$[HONO]_{emis} = K \times [NOx] \tag{1}$$
$$P_{emis} = K \times [\Delta NOx]/\Delta t \tag{2}$$
$$P_{emis} = K \times NOx* \tag{3}$$
$$P_{HONO} = \frac{[HONO]_{t_2} - [HONO]_{t_1}}{t_2 - t_1} \tag{4}$$

In this study, we first used NOx emission rate from a high-resolution emission inventory (Huang et al., 2021) to calculate emission rate of HONO P_{emis} at night (18:00–6:00). The NOx emission rate was extracted from a 3 km × 3 km grid cell centred around our site. As a comparison, we also used the 2017 NOx emission inventory of Guangzhou city to repeat the calculation. The two inventories are primarily different in spatial resolution. The high-resolution 3 km × 3 km data is

255 expected to better represent local traffic emissions, whereas the city-level emission inventory represents the total emission. Since we cannot quantify the relative contribution of the local and regional emissions to this site, two results are used to represent upper and lower limits of the contribution of primary emissions to HONO. The nighttime height of the boundary layer is assuming to 200 m according to the previous study in the PRD region in autumn by Fan et al. (2008).

260 The observed HONO accumulation rate P_{HONO} is calculated by Eq. (4), where $[HONO]_{t_1}$ and $[HONO]_{t_2}$ represent the HONO concentration at 18:00 and 6:00 Local Time, respectively. Then an average P_{HONO} of 0.02 ± 0.06 ppbv h^{-1} can be derived. Hourly HONO primary emission rates calculated with the two inventories are shown in Fig. 5 (a). P_{emis} calculated with the high-resolution emission data (3 km × 3 km) shows a steep downward trend from 18:00 (0.56 ppbv h^{-1}) to 4:00 (0.14 ppbv h^{-1}), followed by an upward trend from 4:00 (0.14 ppbv h^{-1}) to 6:00 (0.25 ppbv h^{-1}) with the average of 0.30 ± 0.15 ppbv h^{-1}.

265 By contrast, P_{emis} with the city level emission data (Guangzhou) is much lower (0.04 ± 0.02 ppbv h^{-1}) and varied smoothly throughout the night. Similar results have been obtained at urban sites (Liu et al., 2020a; Liu et al., 2020b; Gu et al., 2021) and a suburban site (Michoud et al., 2014), while the result at a rural site is much lower (Su et al., 2008b) in the PRD region. The uncertainty of P_{emis} stems from the uncertainty of the inventories (-25%–28%) (Huang et al., 2021). Regardless, direct emission of HONO represents a large HONO source at night along with other sources of HONO that remain to be considered.

270

We also calculated the primary emission's contribution to HONO ($[HONO]_{emis}/[HONO]$) using Method (1) and made comparisons against $[HONO]_{emis}/[HONO]$ ratios obtained previously from urban sites in China (Table S3). The values varied widely from 12% to 52%, with seasonal difference of more than a factor of 2 for the same site, reflecting large variability of HONO emissions spatially and temporally. In comparison, the ratio of $[HONO]_{emis}/[HONO]$ at our site is relatively high at

275 47%, as can be expected from the relatively strong vehicle exhaust emissions near our site.

In addition to traffic emissions, we also estimated the HONO emission rate from soil P_{soil} (ppbv h^{-1}) according to Eq. (5) (Liu et al., 2020a):

$$P_{soil} = \frac{\alpha F_{soil}}{H} \tag{5}$$

280 where F_{soil} is the emission flux (g m^{-2} s^{-1}); H is the height of boundary layer (H, m) and was assumed to be 200 m (Fan et al., 2008); α is the conversion factor ($\alpha = \frac{1 \times 10^9 \times 3600 \times R \times T}{M \times P} = \frac{2.99 \times 10^{13} \times T}{M \times P}$); T is the temperature (K); M is the molecular weight (g mol^{-1}) and P is the atmospheric pressure (Pa). HONO emission flux from soil depends on the temperature, water content and nitrogen nutrient content of soil, which have been considered according to the parameters reported in the literature (Oswald et al., 2013). Since grassland, coniferous forest and tropical rain forest are the typical plants in Guangzhou city area (Wu et

285 al., 2015) and their emission fluxes are comparable (Oswald et al., 2013), emission flux from grassland was adopted to represent the soil HONO emission in Guangzhou. The average nighttime P_{soil} varied from 0.011 to 0.035 ppbv h^{-1}, with a mean value of 0.019 ± 0.009 ppbv h^{-1}. The HONO emission rate from soil at our site is slightly larger than the result

reported in Shijiangzhuang urban area (Liu et al., 2020a) and comparable to that in Beijing urban area (Liu et al., 2020b). A caveat is that the calculation relies on laboratory results and is therefore prone to errors due to any possible inconsistency
290 between laboratory simulations and field observations. Overall, soil emission is a minor source compared to other sources.

3.2.2 NO + OH homogeneous reaction

The reaction between NO and OH acts as the most well known ~~principle~~ homogenous HONO source. It can contribute a substantial fraction to HONO formation when NO and OH concentrations are high (Alicke et al., 2003; Liu et al., 2019b; Wong et al., 2011; Tong et al., 2015; Zhang et al., 2019). Taking the homogeneous Reactions R2 and R5 into account, the
295 net HONO homogeneous production rate can be calculated following Eq. (6):

$$NO + OH \rightarrow HONO \tag{R2}$$
$$HONO + OH \rightarrow NO_2 + H_2O \tag{R5}$$
$$P_{OH+NO}^{net} = k_{NO+OH}[NO][OH] - k_{HONO+OH}[HONO][OH] \tag{6}$$

300

In Eq. (6), k_{NO+OH} (7.2×10^{-12} cm^3 s^{-1}) and $k_{HONO+OH}$ (5.0×10^{-12} cm^3 s^{-1}) are the reaction rate constants of the Reactions R2 and R5 at 298 K, respectively (Li et al., 2012). Since the OH concentration was not measured, an average nighttime value of 0.5×10^6 cm^{-3} measured in Heshan in the PRD region in autumn of 2014 was assumed (Tan et al., 2019). As shown in Fig. 3, the variation of P_{OH+NO}^{net} largely followed that of NO, since the concentration of NO was 10 times larger than HONO. And the
305 average value of P_{OH+NO}^{net} is 0.13 ± 0.30 ppbv h^{-1}, leading to a cumulative HONO contribution of 1.62 ppbv. The obtained P_{OH+NO}^{net} is similar to previous studies, such as 0.12 ppbv h^{-1} in Xianyang (Li et al., 2021), 0.13 ppbv h^{-1} in Zhengzhou (Hao et al., 2020), 0.26 ppbv h^{-1} in Xi'an (Huang et al., 2017) and 0.28 ppbv h^{-1} in Guangzhou Back Garden (Li et al., 2012). We note that the measured HONO only increased 0.26 ppbv in this period, much smaller than the cumulative production of HONO by the reaction between NO and OH, indicating a large sink to balance this source and other sources that will be
310 discussed below.

Since OH was not measured in our study, we carried out sensitivity tests using one fifth and twice of assumed OH concentration (0.5×10^6 cm^{-3}) (Lou et al., 2010). As shown in Table S4, within the range of nighttime OH concentration, the cumulative production of the homogeneous reaction of NO + OH in this study are always large enough to surpass the
315 average measured accumulation of HONO, indicating that the NO + OH source is a major source term regardless of uncertainties in OH concentrations.
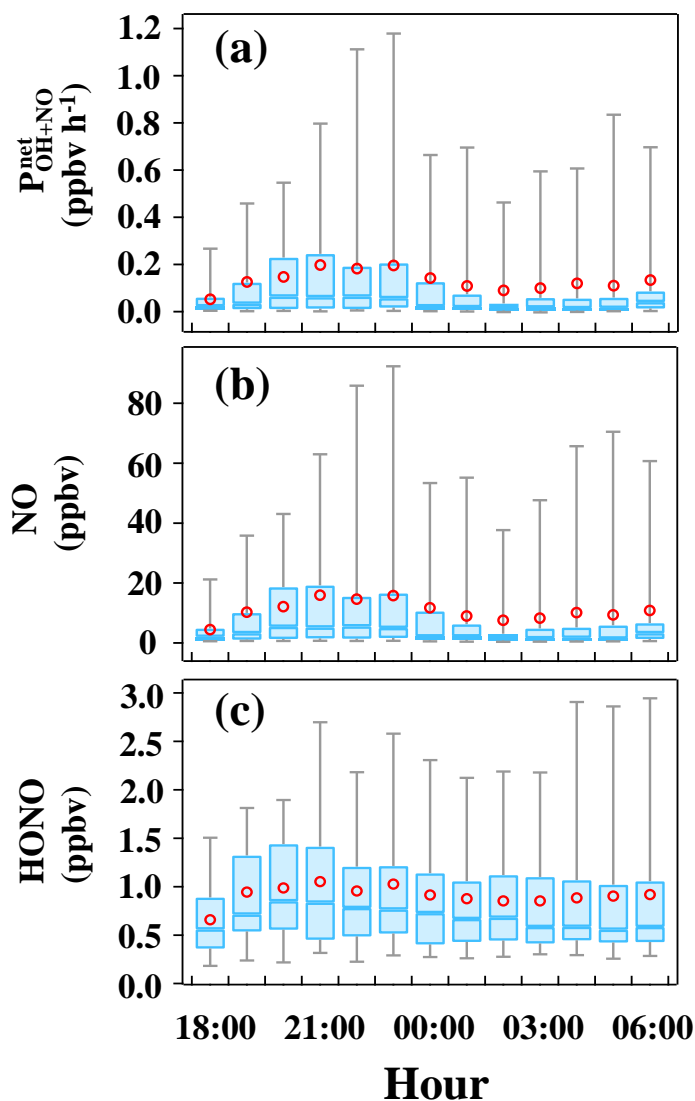
Figure 3. The mean nocturnal variation of (a) P^{net}_{OH+NO}, (b)HONO and NO and (c) HONO. The blue line in the box and red circle refer to the median and mean, respectively. Boxes represent 25% to 75% of the data, and whiskers 95% of the data. Upper and lower boundaries of the box represent the 75th and the 25th percentiles; the whiskers above and below each box represent the 95th and 5th percentiles.

3.2.3 NO₂ to HONO heterogeneous conversion

Our analysis so far suggests that direct emissions and the homogeneous reaction between NO and OH are two major sources of HONO at night. This finding is in line with the relatively high correlation ($R^2 = 0.5927$) between HONO and NO (Fig. 4 (a)). In the following, we present results from correlation analysis to explore possible pathways of heterogeneous NO_2 to HONO conversion at night (18:00–6:00).

The ratio of HONO/NO$_2$ has often been used to indicate the heterogeneous conversion efficiency of NO$_2$ to HONO (Lammel and Cape, 1996; Stutz et al., 2002), for being less influenced by transport processes or convection. Figure 4 (c) shows a weak correlation (R^2 = 0.0638) between HONO/NO$_2$ and PM$_{2.5}$, suggesting that the formation of HONO on aerosol surfaces might not be the main pathway (Kalberer et al., 1999; Kleffmann et al., 2003; Wong et al., 2011; Zhang et al., 2009; Sörgel et al., 2011a; VandenBoer et al., 2013). Because the surface area of ground (including vegetation surface, building surface and soil, etc.) is generally larger than the surface area of aerosols, some studies suggested that the heterogeneous reaction of NO$_2$ and water vapor on ground surfaces was the main source of HONO (Harrison and Kitto, 1994; Li et al., 2012; Wong et al., 2012). Furthermore, the correlations between HONO/NO$_2$ and NH$_3$ and RH are 0.3746 and 0.2381, respectively, and the correlation further improved between HONO/NO$_2$ and the product of NH$_3$ and RH (R^2 = 0.4597). Some studies proposed that NH$_3$ can decrease the free-energy barrier in hydrolysis of NO$_2$ thus enhance the HONO formation (Xu et al., 2019; Li et al., 2018b; ~~Zhang and Tao, 2010~~; Wang et al., 2021a).
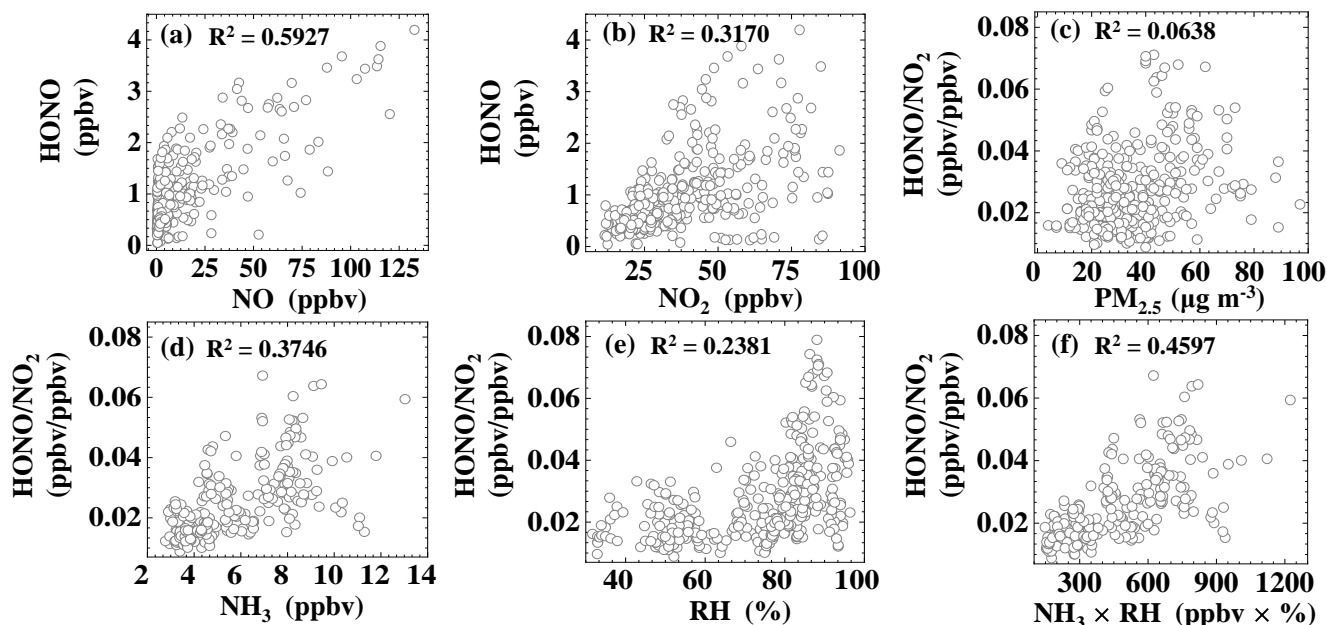
Figure 4. Correlations between HONO, HONO/NO$_2$ and various parameters during the time interval of 18:00–6:00.

In Fig. S5, we further explored the RH effect by focusing on high HONO/NO$_2$ values, i.e., the 5 highest HONO/NO$_2$ values for 5% RH intervals (Stutz et al., 2004). When RH was lower than 87.5%, HONO/NO$_2$ increased with RH, which is in accordance with the reaction kinetics of disproportionation reaction of NO$_2$ and H$_2$O. Furthermore, the slope of linear fitting between HONO/NO$_2$ and RH was much smaller for RH range of 30% ~ 70% (slope = 0.04%; R^2 = 0.5202) than for the RH range of 70% ~ 87.5% (slope = 0.25%, R^2 = 0.8767). Similar piecewise correlations between HONO/NO$_2$ and RH have been found in previous studies (Qin et al., 2009; Zhang et al., 2019), which have been interpreted as evidence for the non-linear

dependence of NO$_2$-to-HONO conversion efficiency on RH. Once the relative humidity exceeded 87.5%, NO$_2$-to-HONO conversion appeared to be inhibited by RH (slope = -0.32%; R^2 = 0.9750). A possible explanation is that the number of water

350 layers formed on various surfaces increased rapidly with RH, resulting in effective uptake of HONO and making the surface inaccessible or less reactive to NO$_2$. Previous studies also found fast growth of aqueous layers when RH over 70% for glass (Saliba et al., 2001) and over 80% for stone (Stutz et al., 2004). The tipping point inferred from ambient observations appear to vary across locales, likely reflecting the different composition of the ground surfaces, e.g., 60% for Chengdu (Yang et al., 2021b), 65–70% for Beijing (Wang et al., 2017a), 70% for Back Garden (Li et al., 2012), 75% for Shanghai (Wang et al.,

355 2013), and 85% for Xi'an (Huang et al., 2017).

We calculated the strength of the HONO formation from NO$_2$ heterogenous reaction on on ground surface (P$_{ground}$) and aerosol surface (P$_{aerosol}$) based on the empirical data derived from either experiments or observations.

$$P_{ground} = \frac{1}{8} \, \gamma_{NO_2 \rightarrow ground} \times [NO_2] \times C_{NO_2} \times \frac{S_g}{V} \tag{7}$$

360
$$P_{aerosol} = \frac{1}{4} \, \gamma_{NO_2 \rightarrow aerosol} \times [NO_2] \times C_{NO_2} \times \frac{S_a}{V} \tag{8}$$

$$\frac{S_g}{V} = \frac{2.2}{H} \tag{9}$$

Where C$_{NO2}$ is the mean molecular velocity of NO$_2$ (m s^{-1}), $\gamma_{NO_2 \rightarrow ground}$ and $\gamma_{NO_2 \rightarrow aerosol}$ represent the uptake coefficient of NO$_2$ on ground surface and aerosol surface, respectively, S$_g$/V and S$_a$/V are the surface area to volume ratio (m^{-1}) for both ground and aerosol, respectively. Considering the land use type of the study site, we treated the ground as an uneven surface,

365 and a factor of 2.2 per unit ground surface measured by Voogt and Oke (1997) was adopted to calculate the total active surface. Hence, S$_g$/V can be calculated by Eq. (9), where H is the mixing layer height. The surface area-to-volume ratio S$_a$/V of PM$_{10}$ was not avaliable in this study and was estimated according to PM$_{2.5}$ and S$_a$/V value in Guangzhou Xinken by Su et al. (2008a). The uptake coefficients of NO$_2$ on ground surface and aerosol surface were assumed to be 4 $\times$ 10^{-6} following previous studies (Li et al., 2018a; Liu et al., 2019a; Zhang et al., 2021) (the summary of the parameterisations used for

370 nighttime HONO budget calculation can be found in Table S5). With these assumptions, an average value of P$_{ground}$ of 0.27 $\pm$ 0.13 ppbv h^{-1} can be derived, which is far larger than P$_{aerosol}$ (0.03 $\pm$ 0.02 ppbv h^{-1}) (Fig. 5 (c) and (d)).

In sum, our correlation analysis for HONO/NO$_2$ and parameterized calculations suggested that nighttime heterogenous conversion of NO$_2$ into HONO at our site maily occured on the ground rather than on aerosol sources, while the correlation

375 analysis provides evidence for the role of NH$_3$ and water vapor in HONO formation. It should be noted that, unlike the NO + OH reaction or the primary emission, which turned out as major HONO sources even at their lower limit considering uncertainties, the magnitude of the heterogenous source as well as its contribution to overall HONO budget varied greatly with the assumed uptake coefficients of NO$_2$, which can span two orders of magnitude.

3.2.4 Removal of HONO

As discussed above, strong sinks are required to balance the nighttime HONO production. Since the reactions of HONO + OH and HONO + HONO are negligible (Kaiser and Wu, 1977; Mebel et al., 1998), it is conceivable that nighttime HONO is mainly removed through deposition L_{Dep} (El Zein and Bedjanian, 2012; Li et al., 2012; Hao et al., 2020; Meng et al., 2020), transport processes, e.g. entrainment of background air $L_{dilution}$ (Gall et al., 2016; Meng et al., 2020), and uptake on aerosols $L_{aerosol}$. These terms can be expressed as follows:

$$L_{Dep} = \frac{V_d \times [HONO]}{H} \tag{10}$$

$$L_{aerosol} = \frac{1}{4} \, \gamma_{HONO \rightarrow aerosol} \times [HONO] \times C_{HONO} \times \frac{S_a}{V} \tag{11}$$

$$L_{dilution} = k_{(dilution)} \times ([HONO] - [HONO]_{background}) \tag{12}$$

where V_d is the average deposition velocity, $\gamma_{HONO \rightarrow aerosol}$ is the uptake coefficient of HONO on aerosol surface, $k_{(dilution)}$ is the dilution rate (including both vertical and horizontal transport) (Dillon et al., 2002). C_{HONO} is the mean molecular velocity of HONO (m s^{-1}), and [HONO] and [HONO]$_{background}$ represents the HONO concentration at the observation site and the background site, respectively. In this work, the lowest nighttime HONO concentration was taken as the [HONO]$_{background}$.

The average loss rate of HONO by dilution was calculated to be 0.18 ± 0.16 ppbv h^{-1}, which is in the range of prior results (Gall et al., 2016; Liu et al., 2020a; Liu et al., 2020b). The average value of $L_{aerosol}$ and $L_{OH+HONO}$ was 0.008 ± 0.006 ppbv h^{-1} and 0.008 ± 0.012 ppbv h^{-1}, respectively. In order to balance the nighttime HONO budget and assuming dry deposition to be responsible for the remaining amount of HONO loss, a dry deposition rate of ~ 2.5 cm s^{-1} was adopted accounting for an average loss rate of 0.41 ± 0.31 ppbv h^{-1} by deposition between 18:00–6:00, when using the median parameter values in Table S5 to calculate the HONO sources and sinks. This result is consistent with previous studies suggesting dry deposition as the dominant loss way for HONO during night (Li et al., 2012; Hao et al., 2020; Meng et al., 2020; VandenBoer et al., 2013). The upper limit of $L_{aerosol}$ is only 0.10 ± 0.08 ppbv h^{-1}, suggesting that HONO loss on aerosols was not a major sink, as also suggested by prior studies (El Zein and Bedjanian, 2012; El Zein et al., 2013; Romanias et al., 2012).

3.2.5 Nighttime HONO budget: relative importance of sources and their uncertainties

It is useful to evaluate the balance of HONO budget by evaluating calculated/parameterized sources and sinks against the observed HONO level and variability. The observed production rate of HONO P_{obs} can be defined as the sum of the total loss rates and change rates of HONO (Gu et al., 2021). When using the median values of parameters (Table S5) and taking an average throughout the night (18:00–6:00), all five sources are greater than or close to the average accumulating rate of

HONO at night derived from observed HONO variation (0.02 ± 0.06 ppbv h^{-1}), indicating a balanced HONO budget considering all uncertainties. Ranking the source strengths with their median estimates suggested that heterogeneous conversion of NO$_2$ on ground surface (0.27 ± 0.13 ppbv h^{-1}), primary emission from vehicle exhaust (between 0.04 ± 0.02 ppbv h^{-1} and 0.30 ± 0.15 ppbv h^{-1} with a middle value of 0.16 ± 0.07 ppbv h^{-1}) and the homogeneous reaction of NO + OH

415   (0.14 ± 0.30 ppbv h^{-1}) were major sources of HONO at night. Nighttime soil emission rate (0.019 ± 0.009 ppbv h^{-1}) and heterogeneous NO$_2$ conversion on the aerosol surfaces (0.03 ± 0.02 ppbv h^{-1}) were two other minor sources. Dry deposition (0.41 ± 0.31 ppbv h^{-1}) was the principal loss process of nighttime HONO, followed by dilution (0.18 ± 0.16 ppbv h^{-1}), while the homogeneous reaction of HONO + OH (0.008 ± 0.012 ppbv h^{-1}) and HONO uptake on the aerosol surfaces (0.008 ± 0.006 ppbv h^{-1}) were insignificant.

420

We also made an attempt to obtain a time resolved HONO budget on an hourly basis, although the results are not satisfactory for all the hours at night, with obvious differences between observed and calculated rates of HONO variation, e.g., at 22:00 and from 2:00 to 5:00 (Fig. S6). This is well expected considering much more amplified uncertainties associated with hourly variabilities of various quantities, which can be considerably reduced by averaging all hours. This is why subtle and careful

425   data filtering is necessary when nightime HONO chemistry is examined in detail (Wong et al., 2011). Such a granular analysis is more appropriate for the daytime when HONO lifetime is much shorter and uncertainties affecting the interpretation of HONO chemistry (e.g., emission and transport) are much muted. As a matter of fact, because the rate of HONO change shown in Fig. S6 is a first order derivative of the HONO concentration itself, one can expect that HONO concentrations from each source would show greater variations, making it more difficult to compare on an hourly basis.

430   Another challenge is that since those parameters used for calculating HONO source strengths have a range in their estimates (Table S5), the HONO source strengths also have a wide range individually, and therefore there are numerous possible combintions of these sources with different strengths and rankings to close the budget.

The comparison and ranking of sources considering variability and uncertainty becomes less straightforward than ranking

435   nighttime average source strengths (Fig. 5). Among the three largest sources, both primary (non-soil) emission and NO$_2$ heterogenous source on ground showed an evening peak and decreased ~~toward~~ after midnight. The NO + OH source showed a different trend with its lowest level in the evening, making it the smallest source among the three at that time. Although the NO$_2$ heterogenous source on ground appeared the largest with its median parameter value, it also had the largest range of estimate, suggesting that its importance is more uncertain compared to the other sources. On the other hand, the other two

440   minor sources, i.e., the NO$_2$ heterogenous source on aerosols and soil emission are substantially less ~~unlikely more~~ important than these three sources given their ranges of low estimates. The variability and uncertainty of dry deposition are entirely ~~largely~~ dependant on other terms of sources and sinks since it is derived as a final term to balance the budget.
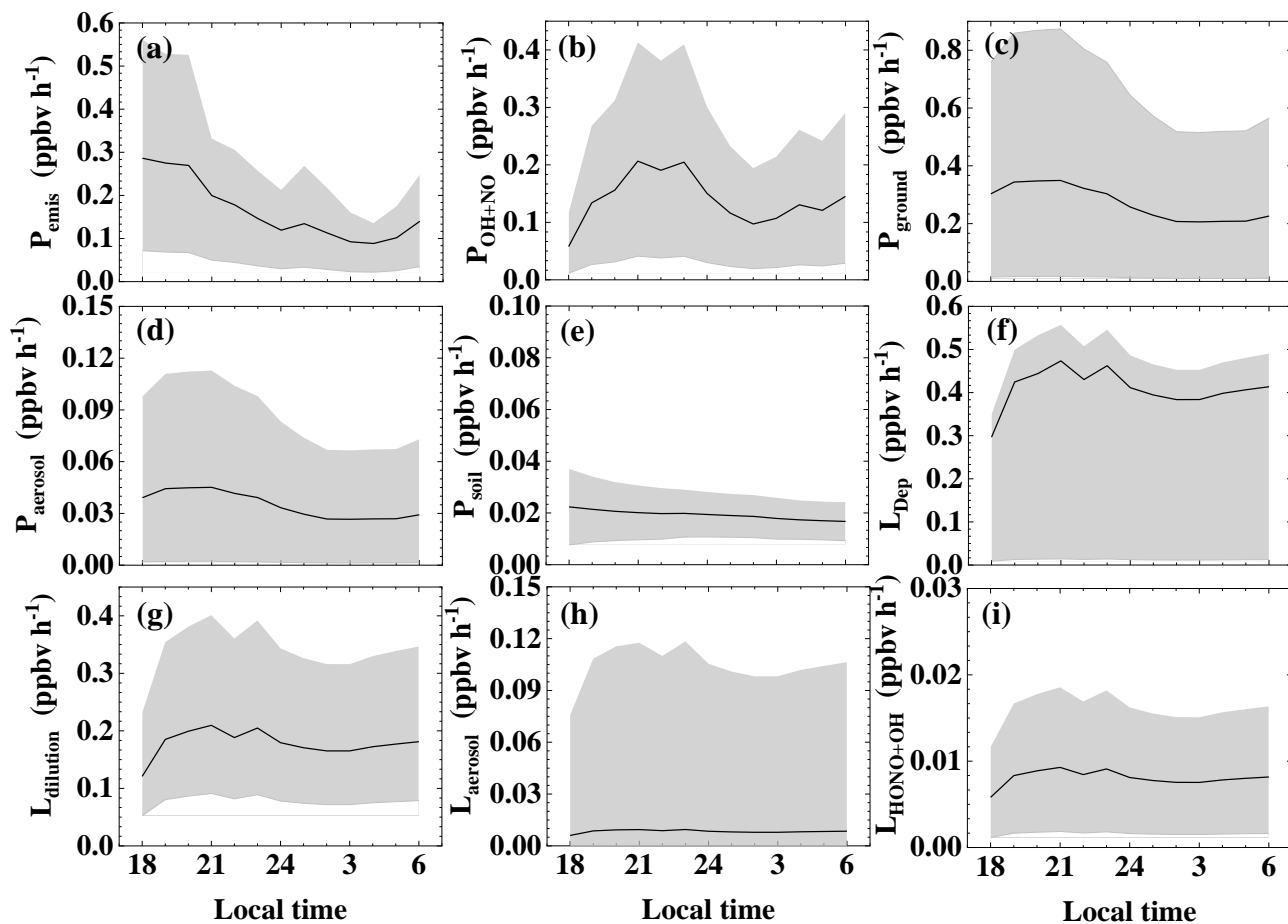
445 **Figure 5. The nocturnal variation of the terms of HONO budget (a) primary emission from vehicle exhaust, (b) homogeneous reaction of NO + OH, (c) heterogeneous conversion of NO₂ on ground surfaces, (d) heterogeneous conversion of NO₂ on aerosol surfaces, (e) soil emission and HONO loss from (f) dry deposition, (g) dilution, (h) uptake on aerosols, (i) HONO + OH during Sep. 27–Nov. 9 2018 in Guangzhou. The black line is the HONO production rates with the median values of parameters, and the grey shadow represents their lower and upper limits.**

450

3.3 Daytime HONO budget and unknown sources analysis

3.3.1 Budget analysis

In this section, we move on to a detailed budget analysis for HONO during the daytime, when chemistry is distinctly different from at night. Similar to the nighttime analysis by exploring ~~envoking~~ different terms for the daytime chemistry, the

455 time variation of HONO concentration at our site can be related to its sources and sinks as follows:

$$\frac{\partial[\text{HONO}]}{\partial t} = P_{\text{HONO}} - L_{\text{HONO}} = (P_{\text{OH+NO}} + P_{\text{Unknown}} + P_{\text{emis}} + P_{\text{soil}} + T_V + T_H) - (L_{\text{OH+HONO}} + L_{\text{Phot}} + L_{\text{Dep}}) \quad (13)$$

where $\partial[\text{HONO}]/\partial t$ represents the time variation of HONO; P_{HONO} and L_{HONO} are the sources and sinks of HONO,
460   respectively; $P_{\text{OH+NO}}$ and $L_{\text{OH+HONO}}$ are the homogeneous HONO formation and loss rates in Reactions R2 and R5,
respectively; P_{Unknown} is the HONO production rate from unknown sources; T_V and T_H are two terms representing vertical
and horizontal transport processes, respectively; L_{Phot} denotes the photolysis loss rate of HONO, which can be calculated
with $L_{\text{Phot}} = J(\text{HONO}) \times [\text{HONO}]$; deposition loss rate of HONO L_{Dep} can be calculated by Eq. (10). Assuming a daytime V_d
of 1.6 cm s^{-1} (Hou et al., 2016; Li et al., 2011) and a daytime mixing height (H) of 1000 m (Liao et al., 2018; Song et al.,
465   2019), the average L_{Dep} is 0.003 ± 0.001 ppbv h^{-1}, three orders of magnitude smaller than L_{Phot} and therefore can be ignored
in the following discussion.

OH was not measured and was calculated with a parameterized approach based on strong correlation between observed OH
radicals and $J(O^1D)$. The parameterization was first proposed by Rohrer and Berresheim (2006) and has been applied by
470   several studies in China (Lu et al., 2013; Lu et al., 2012; Lu et al., 2014). In this study, OH was estimated with observed
$J(O^1D)$ along with parameters from fitting the observed OH radicals and $J(O^1D)$ data in Guangzhou Back Garden by Lu et al.
(2012). The daytime maximum OH concentration was estimated to be 1.3×10^7 cm^{-3}, which is slightly smaller than the daily
peak values of 1.5–2.6×10^7 cm^{-3} observed in summer of Guangzhou by Lu et al. (2012). And the estimated daily average
OH concentration is 6.7×10^6 cm^{-3}, close to 7.5×10^6 cm^{-3} measured in the PRD region in autumn of 2014 by Yang et al.
475   (2017b). Daytime P_{emis} was calculated based on the method (3) (mentioned in Sect. 3.2.1). Because the HONO lifetime was
in the order of 20 min under typical daytime conditions (Stutz et al., 2000) and the transport distance is only a few kilometers,
the NOx emission rate extracted from the 3 km × 3 km grid cell centred around sampling site is used to calculate the impact
of primary emission on HONO.

480   To minimize interferences, we chose a period from 9:00 to 15:00 with intense solar radiation and a short HONO lifetime.
Horizontal transport T_H was assumed negligible by selecting the cases with low wind speed (below 3 m s^{-1}) (Su et al., 2008b;
Yang et al., 2014). The magnitude of vertical transport T_V can be estimated by using a parameterization for dilution by
background air according to Dillon et al. (2002), i.e. $T_V = k_{\text{(dilution)}} \times ([\text{HONO}] - [\text{HONO}]_{\text{background}})$. Where $k_{\text{(dilution)}}$ is the
dilution rate, $[\text{HONO}]_{\text{background}}$ represents the background HONO concentration. Assuming a $k_{\text{(dilution)}}$ of 0.23 h^{-1} (Dillon et al.,
485   2002; Sörgel et al., 2011a), a $[\text{HONO}]_{\text{background}}$ value of 10 pptv (Zhang et al., 2009), and taking the mean noontime [HONO]
value of 400 pptv in this study, a value of about 0.09 ppbv h^{-1} can be derived, which is much smaller than L_{Phot} and can be
ignored in the following discussion. The average daytime HONO emission rate from soil P_{soil} varied from 0.002 to 0.007
with a mean value of 0.004 ± 0.002 ppbv h^{-1}, which is three orders of magnitude smaller than L_{Phot}, and can also be ignored

in the following discussion. As a result, $P_{Unknown}$ can be expressed by Eq. (14), in which $\partial[HONO]/\partial t$ is substituted by
490    $\Delta[HONO]/\Delta t$.

$$\frac{\Delta[HONO]}{\Delta t} = (P_{OH+NO} + P_{emis} + P_{Unknown}) - (L_{OH+HONO} + L_{Phot}) \tag{14}$$

Figure 6 shows the budget of HONO from 9:00 to 15:00. As expected, photolysis HONO L_{Phot} (1.58 ± 0.82 ppbv h^{-1}) was
495   the main loss pathway in the day, followed by a small contribution by the homogeneous reaction of HONO + OH ($L_{OH+HONO}$,
0.07 ± 0.03 ppbv h^{-1}). Among the sources, P_{OH+NO} and $P_{Unknown}$ were comparable in magnitudes, with an average of $0.79 \pm$
0.61 ppbv h^{-1} and 0.65 ± 0.46 ppbv h^{-1}, respectively. $P_{Unknown}$ showed a photo-enhanced feature, reaching its maximum at
12:00 at 0.97 ppbv h^{-1}, similar to the observations in Xinken (Su et al., 2008b), Beijing (Yang et al., 2014), Wangdu (Liu et
al., 2019a), Changzhou (Zheng et al., 2020) and Cyprus (Meusel et al., 2016). The average of $P_{Unknown}$ is comparable to the
500   observation in Back Garden (0.77 ppbv h^{-1}) by Li et al. (2012), but smaller than those in Xinken (≈ 2.0 ppbv h^{-1}) by Su et al.
(2008b) and Guangzhou city area (1.25 ppbv h^{-1}) by Yang et al. (2017a). Homogeneous reaction of NO + OH reached its
maximum in the early morning, and contributed the most fraction in the whole day. Apparently, high NO concentrations at
our site made P_{OH+NO} the biggest daytime source of HONO, exceeding $P_{Unknown}$, similar to observations at other high-NOx
sites such as the Uintah Basin (Tsai et al., 2018), Houston (Wong et al., 2013), Denver (VandenBoer et al., 2013), Santiago
505   de Chile (Elshorbany et al., 2009), London (Heard et al., 2004), Paris (Michoud et al., 2014), Beijing (Liu et al., 2021; Slater
et al., 2020; Zhang et al., 2019; Liu et al., 2020b), Hebei (Xue et al., 2020) and Taiwan (Lin et al., 2006) and Hebei (Xue et
al., 2020). Next, we investigate possible factors relating to $P_{Unknown}$.
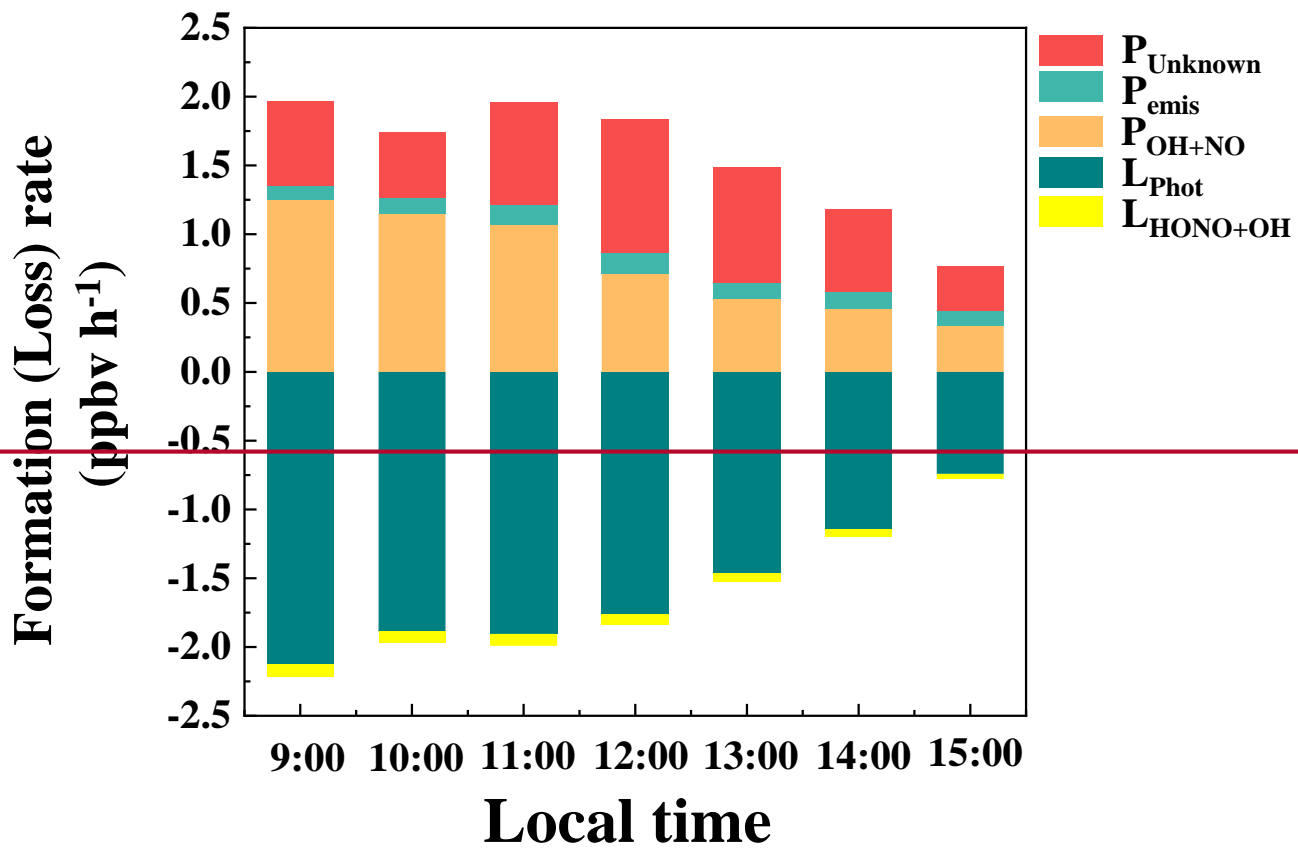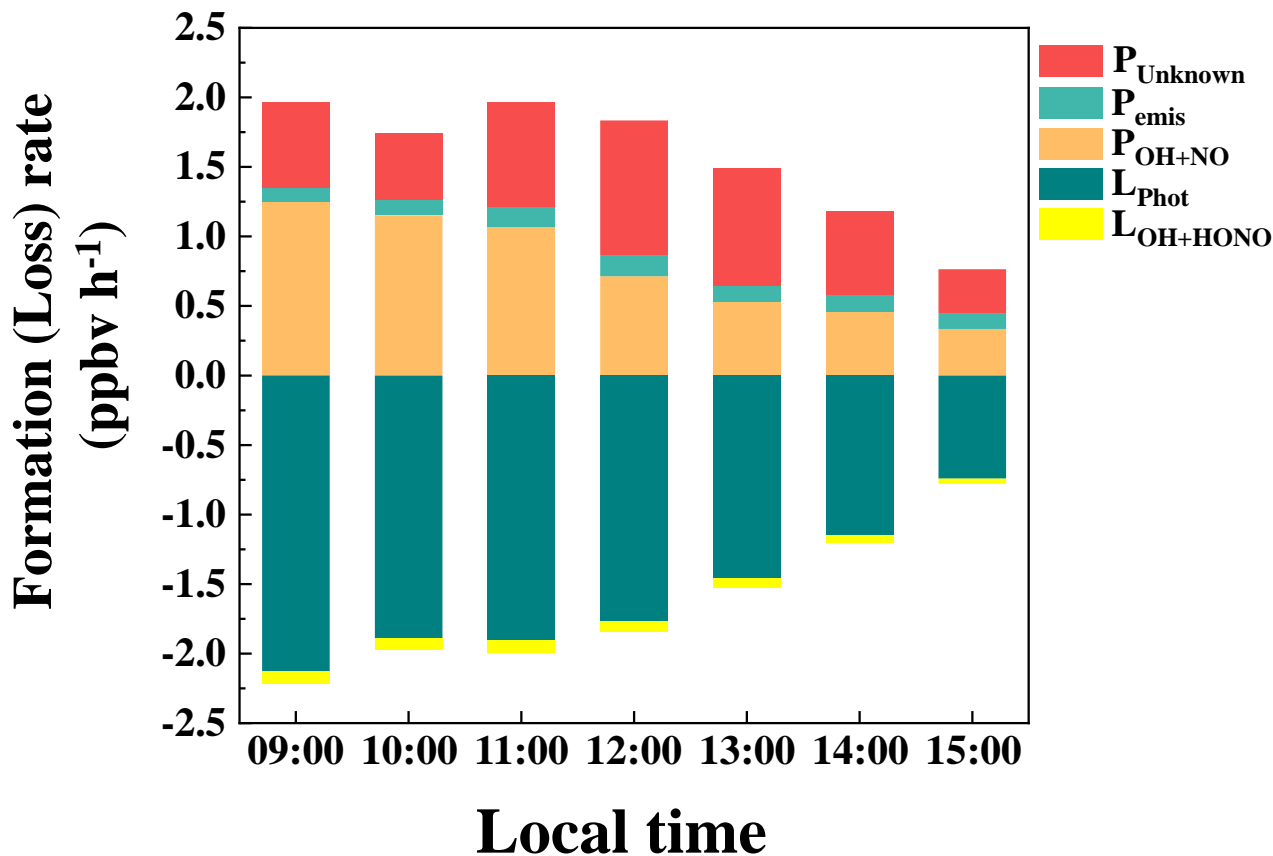
Figure 6. Items of the HONO budget (Eq. (14)) in Guangzhou during the observation period.

~~Figure 7 shows the correlation between $P_{Unknown}$ and NO_2 and $J(NO_2)$ was 0.0681 and 0.2713, respectively. The correlation between $P_{Unknown}$ and $NO_2 \times J(NO_2)$ further improved to 0.4116, indicating that $P_{Unknown}$ may be related to the photo-enhanced reaction of NO_2 (Jiang et al., 2020; Li et al., 2018a; Liu et al., 2019a; Liu et al., 2019b; Su et al., 2008b; Zheng et al., 2020; Huang et al., 2017).~~

3.3.2 Possible mechanisms for daytime HONO production

Figure 7 shows that the correlation between $P_{Unknown}$ and NO_2 and $J(NO_2)$ was 0.0681 and 0.2713, respectively. The correlation between $P_{Unknown}$ and $NO_2 \times J(NO_2)$ further improved to 0.4116, indicating that $P_{Unknown}$ may be related to the photo-enhanced reaction of NO_2 (Jiang et al., 2020; Li et al., 2018a; Liu et al., 2019a; Liu et al., 2019b; Su et al., 2008b; Zheng et al., 2020; Huang et al., 2017). No correlation was found between $P_{Unknown}$ and $PM_{2.5}$ ($R^2 = 0.00014$), indicating that particulate matters may not be a key factor in daytime HONO production (Wong et al., 2012; Li et al., 2018a; Sörgel et al., 2011a; Wang et al., 2017a; Zheng et al., 2020). Meanwhile, the correlations between $P_{Unknown}$ and nitrate in PM_1 and the sum

of gaseous nitric acid and nitrate in PM_1 were very low, with R^2 of 0.0348 and 0.0062 respectively. And the correlation between $P_{Unknown}$ and the product of nitrate and $J(NO_2)$ was also poor (R^2 =~~0.0007~~0.0073), which does not relate $P_{Unknown}$ to the photolysis of nitrate or gaseous nitric acid. Wang et al. (2016) and Ge et al. (2019) suggested that NH_3 can efficiently

525   promote the reaction of NO_2 and SO_2 to form HONO and sulfate. However, we did not find good correlations for $P_{Unknown}$ vs. NH_3, $P_{Unknown}$ vs. SO_2, or $P_{Unknown}$ vs. $NH_3 \times SO_2$.

In summary, at our site with relatively strong traffic impact and high NO, NO + OH appears to be the largest daytime HONO source followed by an unknown photolytic source, which does not seem to be related to aerosols, nor does it seem to be

530   related to the photolysis of nitrate/nitric acid, nor the reaction between NO_2, SO_2 and NH_3.
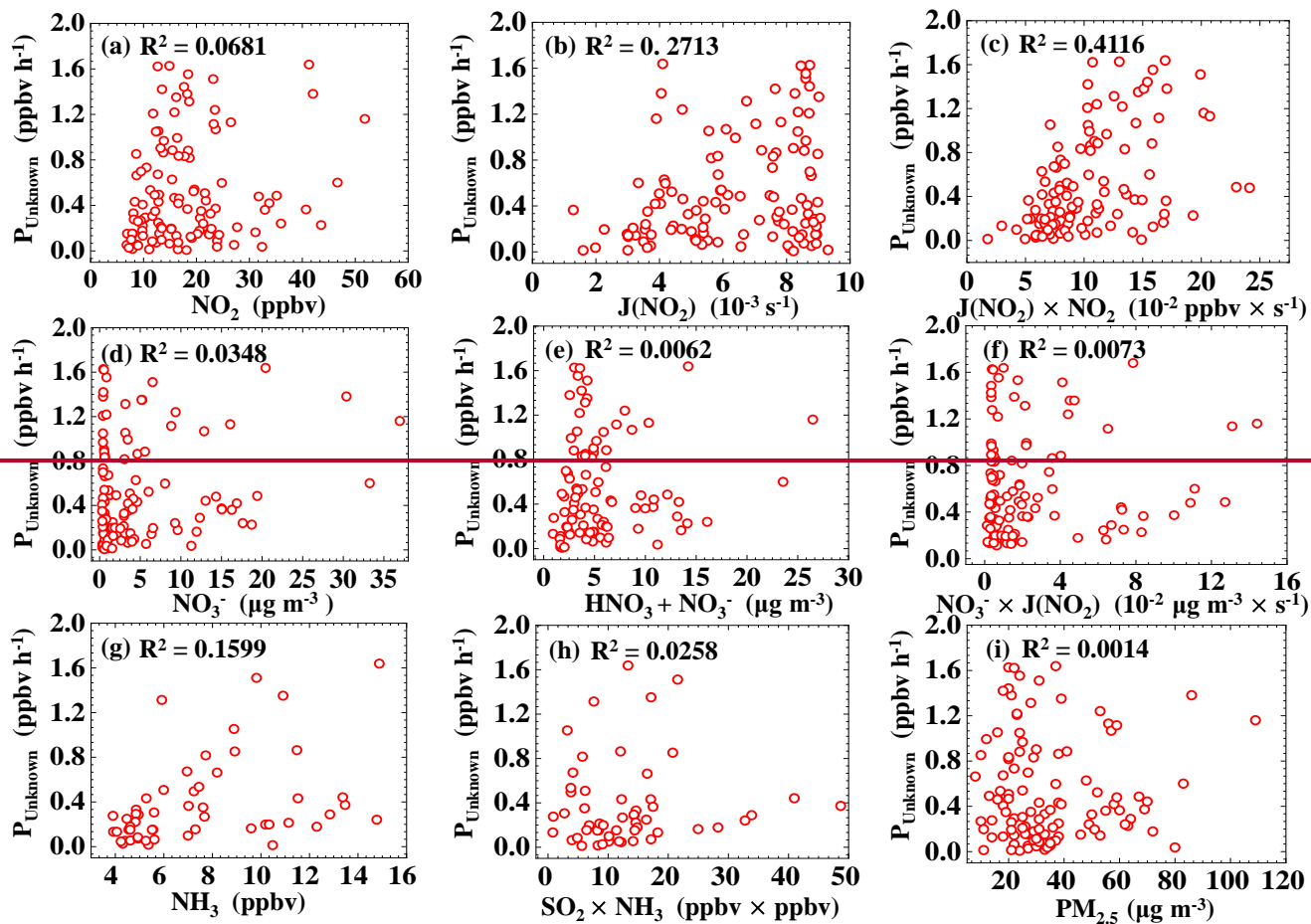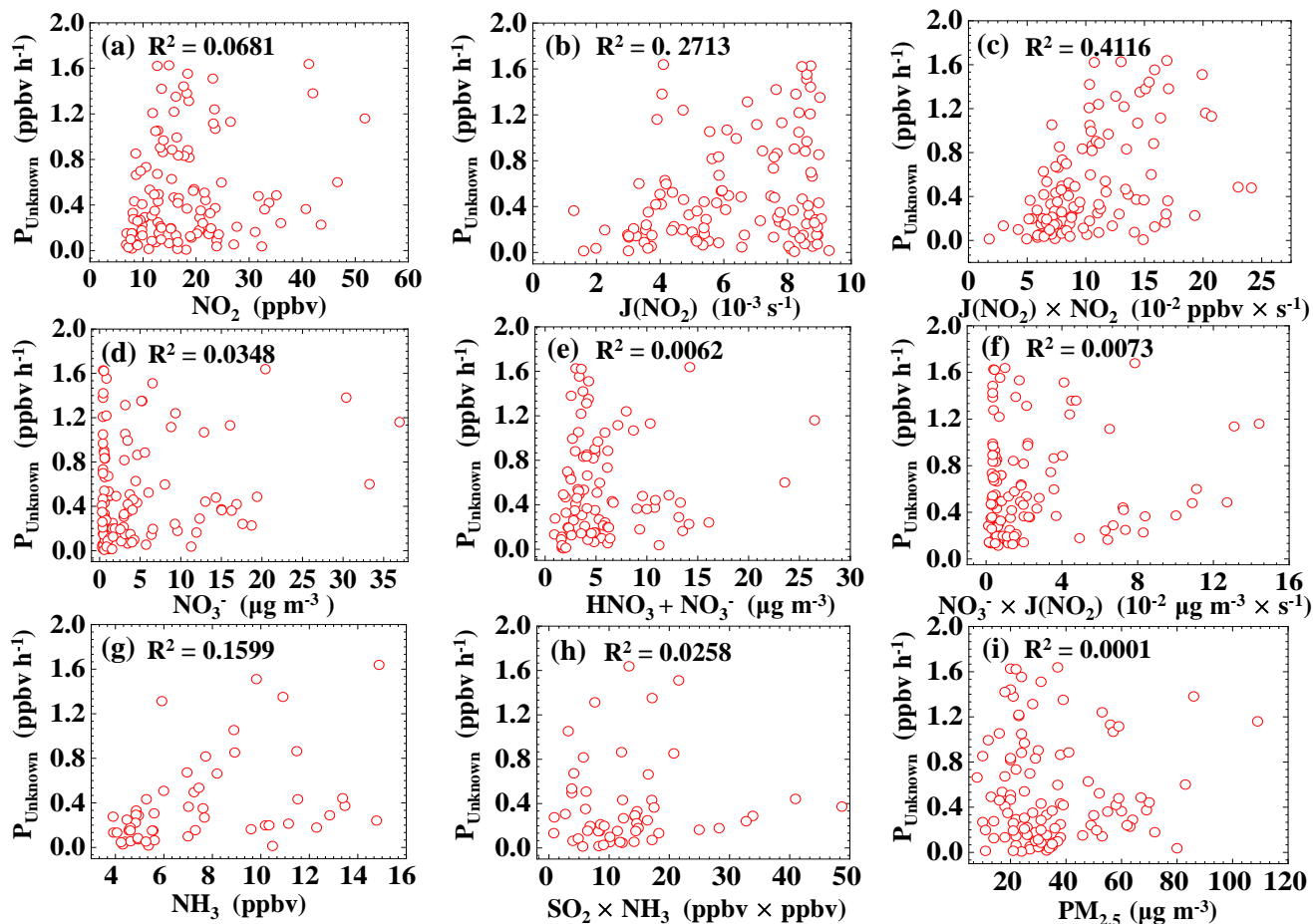
Figure 7. Correlations between daytime HONO unknown sources P_{Unknown} and related parameters.

4 Conclusions

535   Nitrous acid (HONO) was measured with a custom-built LOPAP instrument, along with meteorological parameters and other atmospheric constituents at an urban site in Guangzhou in Pearl River Delta from 27 September to 9 November 2018. The HONO concentrations varied from 0.02 to 4.43 ppbv with an average of 0.74 ± 0.70 ppbv. Compared to prior measurements in Guangzhou, a decreasing trend of HONO can be seen along with improved air quality in the city over the past decade.

540

We have investigated budget of HONO at this site using these data and our key findings are summarized as follows.

We found that the emission ratios (HONO/NOx) derived from an analysis of 11 fresh plumes varied from 0.1% to 1.5% with an average value of 0.9% $\pm$ 0.4%. Using this estimated emission ratio and an estimate of NOx emission rate extracted from a grid cell around our site in a high-resolution (3 km $\times$ 3 km) NOx emission inventory, we estimated a primary HONO emission rate of 0.30 $\pm$ 0.15 ppbv h^{-1}, which turned out far larger (almost by an order of magnitude) than what would be estimated with a city-level NOx emission estimate, which does not adequately represent NOx emission rate specifically for the observation site. Thus, for future analysis of HONO data to properly estimate direct emission of HONO, we suggest that high quality emission data be used to reduce uncertainty. This is especially crucial for a site that receives nearby traffic emissions like ours.

HONO produced by the homogeneous reaction of NO + OH at night was 0.14 $\pm$ 0.30 ppbv h^{-1}, which represents a secondary HONO source. Another major secondary HONO source at night is heterogeneous conversion of NO$_2$ on ground surface (0.27 $\pm$ 0.13 ppbv h^{-1}). Correlation analysis shows that the heterogeneous reaction of NO$_2$ related to NH$_3$ and RH may contribute to the nighttime HONO formation. These two secondary sources and the primary emission from vehicle exhaust (between 0.04 $\pm$ 0.02 ppbv h^{-1} and 0.30 $\pm$ 0.15 ppbv h^{-1} with a median value of 0.16 $\pm$ 0.07 ppbv h^{-1}) were found to be the three largest sources of HONO at night. Because of the large range of those parameter values assumed in their calculations (e.g., the NO$_2$ uptake coefficient that spans two orders of magnitude), the relative importance of the three major sources depends on these assumptions. Soil emission (0.019 $\pm$ 0.009 ppbv h^{-1}) and heterogeneous NO$_2$ conversion on the aerosol surfaces (0.03 $\pm$ 0.02 ppbv h^{-1}) were two other minor sources. Our calculations suggested that dilution acted as a major sink (0.18 $\pm$ 0.16 ppbv h^{-1}), while loss of HONO on the aerosol surfaces played a much less important role. In order to balance the nighttime HONO budget and assuming dry deposition to be responsible for the remaining amount of HONO loss, a dry deposition rate of 2.5 cm s^{-1} is required, equivalent to a loss rate of 0.41 $\pm$ 0.31 ppbv h^{-1}.

Daytime HONO budget analysis revealed that in order to sustain the observed HONO concentration around 450 pptv despite fast photolysis of HONO, an additional unknown source production rate (P$_{Unkonwn}$) of 0.65 $\pm$ 0.46 ppbv h^{-1} was needed, in addition to primary emission P$_{emis}$ at 0.12 $\pm$ 0.02 ppbv h^{-1}, and the homogenous reaction source P$_{OH+NO}$ at 0.79 $\pm$ 0.61 ppbv h^{-1}. It is worth noting that the homogenous HONO source by NO + OH appeared to be a stronger source of HONO than the unknown source (P$_{Unkonwn}$), because of high levels of NO at our site. Correlation analysis between P$_{Unknown}$ and proxies of different mechanisms showed that P$_{Unknown}$ appeared to be photo-enhanced, and yet the mechanism remains unclear. Aerosols did not appear to be as important as ground as a heterogenous reaction media, as suggested by the weak correlation between P$_{Unknown}$ and PM$_{2.5}$. No correlations were found between P$_{Unknown}$ and nitrate/HNO$_3$, NH$_3$, and SO$_2$.

Overall, these results from our study offer a unique perspective on HONO at an urban site receiving heavy traffic emissions in the PRD region. Our budget calculations and comprehensive uncertainty ananlysis suggest that at such locations as ours, HONO direct emissions and NO + OH can become comparable or even surpass other HONO sources that typically receive

greater attention and interest, such as the NO_2 heterogenous source and the unknown daytime photolytic source. Our findings emphasize the need to reduce the uncertainties of both conventional and novel HONO sources and sinks to advance our understanding of this important source of atmospheric OH.

580

Data availability

The data used in this study are available from the corresponding author upon request (chengp@jnu.edu.cn).

Contribution

Peng Cheng organized the field campaign. Yihang Yu and Huirong Li analyzed the data and wrote the paper. All authors
585 contributed to measurements, discussing results, and commenting on the paper. Yihang Yu and Peng Cheng contributed equally to this work.

Competing interests

The authors declare that they have no conflict of interest.

Acknowledgments

590 This work was funded by the National Key Research and Development Program of China (grant nos. 2018YFC0213904, 2017YFC0210104), Science and Technology Plan Projects in Guangzhou (grant no. 201804010115), the Guangdong Natural Science Funds for Distinguished Young Scholar (grant no. 2018B030306037), the Guangdong Innovative and Entrepreneurial Research Team Program (grant no. 2016ZT06N263), and the Special Fund Project for Science and Technology Innovation Strategy of Guangdong Province (grant no. 2019B121205004). We thank Dr. Jörg Kleffmann for
595 his comments and suggestions. We also thank the anonymous referees and the editor, Steven Brown, for their insightful and constructive comments, which helped in improving the paper.

References

Acker, K., Spindler, G., and Brüggemann, E.: Nitrous and nitric acid measurements during the INTERCOMP2000 campaign in Melpitz, Atmospheric Environment, 38, 6497-6505, https://doi.org/10.1016/j.atmosenv.2004.08.030, 2004.
600 Acker, K., Febo, A., Trick, S., Perrino, C., Bruno, P., Wiesen, P., Möller, D., Wieprecht, W., Auel, R., Giusto, M., Geyer, A., Platt, U., and Allegrini, I.: Nitrous acid in the urban area of Rome, Atmospheric Environment, 40, 3123-3133, https://doi.org/10.1016/j.atmosenv.2006.01.028, 2006.

Alicke, B., Geyer, A., Hofzumahaus, A., Holland, F., Konrad, S., Pätz, H. W., Schäfer, J., Stutz, J., Volz-Thomas, A., and Platt, U.: OH formation by HONO photolysis during the BERLIOZ experiment, Journal of Geophysical Research: Atmospheres, 108, 8247, https://doi.org/10.1029/2001JD000579, 2003.

Ammann, M., Kalberer, M., Jost, D. T., Tobler, L., Rössler, E., Piguet, D., Gäggeler, H. W., and Baltensperger, U.: Heterogeneous production of nitrous acid on soot in polluted air masses, Nature, 395, 157-160, https://doi.org/10.1038/25965, 1998.

Aubin, D. G., and Abbatt, J. P. D.: Interaction of NO_2 with Hydrocarbon Soot: Focus on HONO Yield, Surface Modification, and Mechanism, The Journal of Physical Chemistry A, 111, 6263-6273, https://doi.org/10.1021/jp068884h, 2007.

Bejan, I., Abd-el-Aal, Y., Barnes, I., Benter, T., Bohn, B., Wiesen, P., and Kleffmann, J.: The photolysis of ortho-nitrophenols: a new gas phase source of HONO, Phys Chem Chem Phys, 8, 2028-2035, http://dx.doi.org/10.1039/B516590C, 2006.

Chan, C. K., and Yao, X.: Air pollution in mega cities in China, Atmospheric Environment, 42, 1-42, https://doi.org/10.1016/j.atmosenv.2007.09.003, 2008.

Colussi, A. J., Enami, S., Yabushita, A., Hoffmann, M. R., Liu, W.-G., Mishra, H., and Goddard, I. I. I. W. A.: Tropospheric aerosol as a reactive intermediate, Faraday Discussions, 165, 407-420, http://dx.doi.org/10.1039/C3FD00040K, 2013.

Cui, L., Li, R., Zhang, Y., Meng, Y., Fu, H., and Chen, J.: An observational study of nitrous acid (HONO) in Shanghai, China: The aerosol impact on HONO formation during the haze episodes, Science of The Total Environment, 630, 1057-1070, https://doi.org/10.1016/j.scitotenv.2018.02.063, 2018.

Dillon, M. B., Lamanna, M. S., Schade, G. W., Goldstein, A. H., and Cohen, R. C.: Chemical evolution of the Sacramento urban plume: Transport and oxidation, Journal of Geophysical Research: Atmospheres, 107, ACH 3-1-ACH 3-15, https://doi.org/10.1029/2001JD000969, 2002.

El Zein, A., and Bedjanian, Y.: Reactive Uptake of HONO to TiO2 Surface: "Dark" Reaction, The Journal of Physical Chemistry A, 116, 3665-3672, https://doi.org/10.1021/jp300859w, 2012.

El Zein, A., Romanias, M. N., and Bedjanian, Y.: Kinetics and Products of Heterogeneous Reaction of HONO with Fe2O3 and Arizona Test Dust, Environmental Science & Technology, 47, 6325-6331, https://doi.org/10.1021/es400794c, 2013.

Elshorbany, Y. F., Kurtenbach, R., Wiesen, P., Lissi, E., Rubio, M., Villena, G., Gramsch, E., Rickard, A. R., Pilling, M. J., and Kleffmann, J.: Oxidation capacity of the city air of Santiago, Chile, Atmos. Chem. Phys., 9, 2257-2273, https://doi.org/10.5194/acp-9-2257-2009, 2009.

Fan, S., Wang, B., Tesche, M., Engelmann, R., Althausen, A., Liu, J., Zhu, W., Fan, Q., Li, M., Ta, N., Song, L., and Leong, K.: Meteorological conditions and structures of atmospheric boundary layer in October 2004 over Pearl River Delta area, Atmospheric Environment, 42, 6174-6186, https://doi.org/10.1016/j.atmosenv.2008.01.067, 2008.

Febo, A., Perrino, C., and Allegrini, I.: Measurement of nitrous acid in milan, italy, by doas and diffusion denuders, Atmospheric Environment, 30, 3599-3609, https://doi.org/10.1016/1352-2310(96)00069-6, 1996.

Feng, Y., Ning, M., Lei, Y., Sun, Y., Liu, W., and Wang, J.: Defending blue sky in China: Effectiveness of the "Air Pollution Prevention and Control Action Plan" on air quality improvements from 2013 to 2017, Journal of Environmental Management, 252, 109603, https://doi.org/10.1016/j.jenvman.2019.109603, 2019.

Finlayson-Pitts, B. J., and Pitts, J. N.: CHAPTER 4 - Photochemistry of Important Atmospheric Species, in: Chemistry of the Upper and Lower Atmosphere, edited by: Finlayson-Pitts, B. J., and Pitts, J. N., Academic Press, San Diego, 86-129, 2000.

Finlayson-Pitts, B. J., Wingen, L. M., Sumner, A. L., Syomin, D., and Ramazan, K. A.: The heterogeneous hydrolysis of NO2 in laboratory systems and in outdoor and indoor atmospheres: An integrated mechanism, Physical Chemistry Chemical Physics, 5, 223-242, http://dx.doi.org/10.1039/B208564J, 2003.

Gall, E. T., Griffin, R. J., Steiner, A. L., Dibb, J., Scheuer, E., Gong, L., Rutter, A. P., Cevik, B. K., Kim, S., Lefer, B., and Flynn, J.: Evaluation of nitrous acid sources and sinks in urban outflow, Atmospheric Environment, 127, 272-282, https://doi.org/10.1016/j.atmosenv.2015.12.044, 2016.

Ge, S., Wang, G., Zhang, S., Li, D., Xie, Y., Wu, C., Yuan, Q., Chen, J., and Zhang, H.: Abundant NH_3 in China Enhances Atmospheric HONO Production by Promoting the Heterogeneous Reaction of SO_2 with NO_2, Environ Sci Technol, 53, 14339-14347, https://doi.org/10.1021/acs.est.9b04196, 2019.

Gen, M., Zhang, R., and Chan, C. K.: Nitrite/Nitrous Acid Generation from the Reaction of Nitrate and Fe(II) Promoted by Photolysis of Iron–Organic Complexes, Environmental Science & Technology, 55, 15715-15723, https://doi.org/10.1021/acs.est.1c05641, 2021.

Gerecke, A., Thielmann, A., Gutzwiller, L., and Rossi, M. J.: The chemical kinetics of HONO formation resulting from heterogeneous interaction of NO2 with flame soot, Geophysical Research Letters, 25, 2453-2456, https://doi.org/10.1029/98GL01796, 1998.

Gu, R., Shen, H., Xue, L., Wang, T., Gao, J., Li, H., Liang, Y., Xia, M., Yu, C., Liu, Y., and Wang, W.: Investigating the sources of atmospheric nitrous acid (HONO) in the megacity of Beijing, China, Science of The Total Environment, 152270, https://doi.org/10.1016/j.scitotenv.2021.152270, 2021.

Gutzwiller, L., Arens, F., Baltensperger, U., Gäggeler, H. W., and Ammann, M.: Significance of Semivolatile Diesel Exhaust Organics for Secondary HONO Formation, Environmental Science & Technology, 36, 677-682, https://doi.org/10.1021/es015673b, 2002.

Han, C., Liu, Y., and He, H.: Heterogeneous reaction of NO2 with soot at different relative humidity, Environmental Science and Pollution Research, 24, 21248-21255, https://doi.org/10.1007/s11356-017-9766-y, 2017a.

Han, C., Yang, W., Yang, H., and Xue, X.: Enhanced photochemical conversion of NO2 to HONO on humic acids in the presence of benzophenone, Environmental Pollution, 231, 979-986, https://doi.org/10.1016/j.envpol.2017.08.107, 2017b.

Hao, Q., Jiang, N., Zhang, R., Yang, L., and Li, S.: Characteristics, sources, and reactions of nitrous acid during winter at an urban site in the Central Plains Economic Region in China, Atmos. Chem. Phys., 20, 7087-7102, https://doi.org/10.5194/acp-20-7087-2020, 2020.

Harrison, R. M., and Kitto, A.-M. N.: Evidence for a surface source of atmospheric nitrous acid, Atmospheric Environment, 28, 1089-1094, https://doi.org/10.1016/1352-2310(94)90286-0, 1994.

Heard, D. E., Carpenter, L. J., Creasey, D. J., Hopkins, J. R., Lee, J. D., Lewis, A. C., Pilling, M. J., Seakins, P. W., Carslaw, N., and Emmerson, K. M.: High levels of the hydroxyl radical in the winter urban troposphere, Geophysical Research Letters, 31, https://doi.org/10.1029/2004GL020544, 2004.

Heland, J., Kleffmann, J., Kurtenbach, R., and Wiesen, P.: A New Instrument To Measure Gaseous Nitrous Acid (HONO) in the Atmosphere, Environmental Science & Technology, 35, 3207-3212, https://doi.org/10.1021/es000303t, 2001.

Hendrick, F., Müller, J. F., Clémer, K., Wang, P., De Mazière, M., Fayt, C., Gielen, C., Hermans, C., Ma, J. Z., Pinardi, G., Stavrakou, T., Vlemmix, T., and Van Roozendael, M.: Four years of ground-based MAX-DOAS observations of HONO and NO2 in the Beijing area, Atmos. Chem. Phys., 14, 765-781, https://doi.org/10.5194/acp-14-765-2014, 2014.

Hofzumahaus, A., Rohrer, F., Lu, K., Bohn, B., Brauers, T., Chang, C.-C., Fuchs, H., Holland, F., Kita, K., Kondo, Y., Li, X., Lou, S., Shao, M., Zeng, L., Wahner, A., and Zhang, Y.: Amplified Trace Gas Removal in the Troposphere, Science, 324, 1702-1704, https://doi.org/10.1126/science.1164566, 2009.

Hou, S., Tong, S., Ge, M., and An, J.: Comparison of atmospheric nitrous acid during severe haze and clean periods in Beijing, China, Atmospheric Environment, 124, 199-206, https://doi.org/10.1016/j.atmosenv.2015.06.023, 2016.

Hu, M., Zhou, F., Shao, K., Zhang, Y., Tang, X., and Slanina, J.: Diurnal variations of aerosol chemical compositions and related gaseous pollutants in Beijing and Guangzhou, J Environ Sci Health A Tox Hazard Subst Environ Eng, 37, 479-488, https://doi.org/10.1081/ESE-120003229, 2002.

Huang, R. J., Yang, L., Cao, J., Wang, Q., Tie, X., Ho, K. F., Shen, Z., Zhang, R., Li, G., Zhu, C., Zhang, N., Dai, W., Zhou, J., Liu, S., Chen, Y., Chen, J., and O'Dowd, C. D.: Concentration and sources of atmospheric nitrous acid (HONO) at an urban site in Western China, Science of The Total Environment, 593-594, 165-172, https://doi.org/10.1016/j.scitotenv.2017.02.166, 2017.

Huang, Z., Zhong, Z., Sha, Q., Xu, Y., Zhang, Z., Wu, L., Wang, Y., Zhang, L., Cui, X., Tang, M., Shi, B., Zheng, C., Li, Z., Hu, M., Bi, L., Zheng, J., and Yan, M.: An updated model-ready emission inventory for Guangdong Province by incorporating big data and mapping onto multiple chemical mechanisms, Science of The Total Environment, 769, 144535, https://doi.org/10.1016/j.scitotenv.2020.144535, 2021.

700   Jia, C., Tong, S., Zhang, W., Zhang, X., Li, W., Wang, Z., Wang, L., Liu, Z., Hu, B., Zhao, P., and Ge, M.: Pollution characteristics and potential sources of nitrous acid (HONO) in early autumn 2018 of Beijing, Science of The Total Environment, 735, 139317, https://doi.org/10.1016/j.scitotenv.2020.139317, 2020.

Jiang, Y., Xue, L., Gu, R., Jia, M., Zhang, Y., Wen, L., Zheng, P., Chen, T., Li, H., Shan, Y., Zhao, Y., Guo, Z., Bi, Y., Liu, H., Ding, A., Zhang, Q., and Wang, W.: Sources of nitrous acid (HONO) in the upper boundary layer and lower free troposphere of the North China Plain: insights from the Mount Tai Observatory, Atmos. Chem. Phys., 20, 12115-12131,
705   https://doi.org/10.5194/acp-20-12115-2020, 2020.

Kaiser, E. W., and Wu, C. H.: A kinetic study of the gas phase formation and decomposition reactions of nitrous acid, The Journal of Physical Chemistry, 81, 1701-1706, https://doi.org/10.1021/j100533a001, 1977.

Kalberer, M., Ammann, M., Arens, F., Gäggeler, H. W., and Baltensperger, U.: Heterogeneous formation of nitrous acid (HONO) on soot aerosol particles, Journal of Geophysical Research: Atmospheres, 104, 13825-13832,
710   https://doi.org/10.1029/1999JD900141, 1999.

Kinugawa, T., Enami, S., Yabushita, A., Kawasaki, M., Hoffmann, M. R., and Colussi, A. J.: Conversion of gaseous nitrogen dioxide to nitrate and nitrite on aqueous surfactants, Physical Chemistry Chemical Physics, 13, 5144-5149, http://dx.doi.org/10.1039/C0CP01497D, 2011.

Kirchstetter, T. W., Harley, R. A., and Littlejohn, D.: Measurement of Nitrous Acid in Motor Vehicle Exhaust,
715   Environmental Science & Technology, 30, 2843-2849, https://doi.org/10.1021/es960135y, 1996.

Kleffmann, J., Kurtenbach, R., Lörzer, J., Wiesen, P., Kalthoff, N., Vogel, B., and Vogel, H.: Measured and simulated vertical profiles of nitrous acid—Part I: Field measurements, Atmospheric Environment, 37, 2949-2955, https://doi.org/10.1016/S1352-2310(03)00242-5, 2003.

Kleffmann, J., Gavriloaiei, T., Hofzumahaus, A., Holland, F., Koppmann, R., Rupp, L., Schlosser, E., Siese, M., and
720   Wahner, A.: Daytime formation of nitrous acid: A major source of OH radicals in a forest, Geophysical Research Letters, 32, https://doi.org/10.1029/2005GL022524, 2005.

Kleffmann, J., Lörzer, J. C., Wiesen, P., Kern, C., Trick, S., Volkamer, R., Rodenas, M., and Wirtz, K.: Intercomparison of the DOAS and LOPAP techniques for the detection of nitrous acid (HONO), Atmospheric Environment, 40, 3640-3652, https://doi.org/10.1016/j.atmosenv.2006.03.027, 2006.

725   Kramer, L. J., Crilley, L. R., Adams, T. J., Ball, S. M., Pope, F. D., and Bloss, W. J.: Nitrous acid (HONO) emissions under real-world driving conditions from vehicles in a UK road tunnel, Atmos. Chem. Phys., 20, 5231-5248, https://doi.org/10.5194/acp-20-5231-2020, 2020.

Kurtenbach, R., Becker, K. H., Gomes, J. A. G., Kleffmann, J., Lörzer, J. C., Spittler, M., Wiesen, P., Ackermann, R., Geyer, A., and Platt, U.: Investigations of emissions and heterogeneous formation of HONO in a road traffic tunnel,
730   Atmospheric Environment, 35, 3385-3394, https://doi.org/10.1016/S1352-2310(01)00138-8, 2001.

Lammel, G., and Cape, J. N.: Nitrous acid and nitrite in the atmosphere, Chemical Society Reviews, 25, 361-369, http://dx.doi.org/10.1039/CS9962500361, 1996.

Lee, J. D., Whalley, L. K., Heard, D. E., Stone, D., Dunmore, R. E., Hamilton, J. F., Young, D. E., Allan, J. D., Laufs, S., and Kleffmann, J.: Detailed budget analysis of HONO in central London reveals a missing daytime source, Atmos. Chem.
735   Phys., 16, 2747-2764, https://doi.org/10.5194/acp-16-2747-2016, 2016.

Lelieveld, J., Gromov, S., Pozzer, A., and Taraborrelli, D.: Global tropospheric hydroxyl distribution, budget and reactivity, Atmos. Chem. Phys., 16, 12477-12493, https://doi.org/10.5194/acp-16-12477-2016, 2016.

Li, D., Xue, L., Wen, L., Wang, X., Chen, T., Mellouki, A., Chen, J., and Wang, W.: Characteristics and sources of nitrous acid in an urban atmosphere of northern China: Results from 1-yr continuous observations, Atmospheric
740   Environment, 182, 296-306, https://doi.org/10.1016/j.atmosenv.2018.03.033, 2018a.

Li, J., Lu, K., Lv, W., Li, J., Zhong, L., Ou, Y., Chen, D., Huang, X., and Zhang, Y.: Fast increasing of surface ozone concentrations in Pearl River Delta characterized by a regional air quality monitoring network during 2006–2011, Journal of Environmental Sciences, 26, 23-36, https://doi.org/10.1016/S1001-0742(13)60377-0, 2014a.

Li, L., Duan, Z., Li, H., Zhu, C., Henkelman, G., Francisco, J. S., and Zeng, X. C.: Formation of HONO from the NH_3
745   promoted hydrolysis of NO_2 dimers in the atmosphere, Proceedings of the National Academy of Sciences, 115, 7236-7241, https://doi.org/10.1073/pnas.1807719115, 2018b.

Li, S., Matthews, J., and Sinha, A.: Atmospheric hydroxyl radical production from electronically excited NO_2 and H_2O, Science, 319, 1657-1660, https://doi.org/10.1126/science.1151443, 2008.

Li, W., Tong, S., Cao, J., Su, H., Zhang, W., Wang, L., Jia, C., Zhang, X., Wang, Z., Chen, M., and Ge, M.: Comparative observation of atmospheric nitrous acid (HONO) in Xi'an and Xianyang located in the GuanZhong basin of western China, Environmental Pollution, 289, 117679, https://doi.org/10.1016/j.envpol.2021.117679, 2021.

Li, X., Brauers, T., Häseler, R., Bohn, B., Fuchs, H., Hofzumahaus, A., Holland, F., Lou, S., Lu, K. D., Rohrer, F., Hu, M., Zeng, L. M., Zhang, Y. H., Garland, R. M., Su, H., Nowak, A., Wiedensohler, A., Takegawa, N., Shao, M., and Wahner, A.: Exploring the atmospheric chemistry of nitrous acid (HONO) at a rural site in Southern China, Atmos. Chem. Phys., 12, 1497-1513, https://doi.org/10.5194/acp-12-1497-2012, 2012.

Li, X., Rohrer, F., Hofzumahaus, A., Brauers, T., Häseler, R., Bohn, B., Broch, S., Fuchs, H., Gomm, S., Holland, F., Jäger, J., Kaiser, J., Keutsch, F. N., Lohse, I., Lu, K., Tillmann, R., Wegener, R., Wolfe, G. M., Mentel, T. F., Kiendler-Scharr, A., and Wahner, A.: Missing Gas-Phase Source of HONO Inferred from Zeppelin Measurements in the Troposphere, Science, 344, 292-296, https://doi.org/10.1126/science.1248999, 2014b.

Li, Y., An, J., Min, M., Zhang, W., Wang, F., and Xie, P.: Impacts of HONO sources on the air quality in Beijing, Tianjin and Hebei Province of China, Atmospheric Environment, 45, 4735-4744, https://doi.org/10.1016/j.atmosenv.2011.04.086, 2011.

Liao, B., Huang, J., Wang, C., Weng, J., Li, L., Cai, H., and D, W.: Comparative analysis on the boundary layer features of haze processes and cleaning process in Guangzhou, China Environmental Science, 38, 4432-4443, http://www.zghjkx.com.cn/CN/Y2018/V38/I12/4432, 2018.

Liao, W., Wu, L., Zhou, S., Wang, X., and Chen, D.: Impact of Synoptic Weather Types on Ground-Level Ozone Concentrations in Guangzhou, China, Asia-Pacific Journal of Atmospheric Sciences, https://doi.org/10.1007/s13143-020-00186-2, 2020.

Lin, Y.-C., Cheng, M.-T., Ting, W.-Y., and Yeh, C.-R.: Characteristics of gaseous HNO_2, HNO_3, NH_3 and particulate ammonium nitrate in an urban city of Central Taiwan, Atmospheric Environment, 40, 4725-4733, https://doi.org/10.1016/j.atmosenv.2006.04.037, 2006.

Liu, J., Liu, Z., Ma, Z., Yang, S., Yao, D., Zhao, S., Hu, B., Tang, G., Sun, J., Cheng, M., Xu, Z., and Wang, Y.: Detailed budget analysis of HONO in Beijing, China: Implication on atmosphere oxidation capacity in polluted megacity, Atmospheric Environment, 244, 117957, https://doi.org/10.1016/j.atmosenv.2020.117957, 2021.

Liu, Y.: Observations and parameterized modelling of ambient nitrous acid (HONO) in the megacity areas of the eastern China, Ph.D. thsis. College of Environmental Sciences and Engineering, Peking University, China, 2017.

Liu, Y., Lu, K., Ma, Y., Yang, X., Zhang, W., Wu, Y., Peng, J., Shuai, S., Hu, M., and Zhang, Y.: Direct emission of nitrous acid (HONO) from gasoline cars in China determined by vehicle chassis dynamometer experiments, Atmospheric Environment, 169, 89-96, https://doi.org/10.1016/j.atmosenv.2017.07.019, 2017.

Liu, Y., Lu, K., Li, X., Dong, H., Tan, Z., Wang, H., Zou, Q., Wu, Y., Zeng, L., Hu, M., Min, K. E., Kecorius, S., Wiedensohler, A., and Zhang, Y.: A Comprehensive Model Test of the HONO Sources Constrained to Field Measurements at Rural North China Plain, Environ Sci Technol, https://doi.org/10.1021/acs.est.8b06367, 2019a.

Liu, Y., Nie, W., Xu, Z., Wang, T., Wang, R., Li, Y., Wang, L., Chi, X., and Ding, A.: Semi-quantitative understanding of source contribution to nitrous acid (HONO) based on 1 year of continuous observation at the SORPES station in eastern China, Atmos. Chem. Phys., 19, 13289-13308, https://doi.org/10.5194/acp-19-13289-2019, 2019b.

Liu, Y., Ni, S., Jiang, T., Xing, S., Zhang, Y., Bao, X., Feng, Z., Fan, X., Zhang, L., and Feng, H.: Influence of Chinese New Year overlapping COVID-19 lockdown on HONO sources in Shijiazhuang, Science of The Total Environment, 745, 141025, https://doi.org/10.1016/j.scitotenv.2020.141025, 2020a.

Liu, Y., Zhang, Y., Lian, C., Yan, C., Feng, Z., Zheng, F., Fan, X., Chen, Y., Wang, W., Chu, B., Wang, Y., Cai, J., Du, W., Daellenbach, K. R., Kangasluoma, J., Bianchi, F., Kujansuu, J., Petäjä, T., Wang, X., Hu, B., Wang, Y., Ge, M., He, H., and Kulmala, M.: The promotion effect of nitrous acid on aerosol formation in wintertime in Beijing: the possible contribution of traffic-related emissions, Atmos. Chem. Phys., 20, 13023-13040, https://doi.org/10.5194/acp-20-13023-2020, 2020b.

Liu, Z., Wang, Y., Costabile, F., Amoroso, A., Zhao, C., Huey, L. G., Stickel, R., Liao, J., and Zhu, T.: Evidence of aerosols as a media for rapid daytime HONO production over China, Environ Sci Technol, 48, 14386-14391, https://doi.org/10.1021/es504163z, 2014.

Lou, S., Holland, F., Rohrer, F., Lu, K., Bohn, B., Brauers, T., Chang, C. C., Fuchs, H., Häseler, R., Kita, K., Kondo, Y., Li, X., Shao, M., Zeng, L., Wahner, A., Zhang, Y., Wang, W., and Hofzumahaus, A.: Atmospheric OH reactivities in the Pearl

River Delta – China in summer 2006: measurement and model results, Atmos. Chem. Phys., 10, 11243-11260, https://doi.org/10.5194/acp-10-11243-2010, 2010.

Lu, K. D., Rohrer, F., Holland, F., Fuchs, H., Bohn, B., Brauers, T., Chang, C. C., Häseler, R., Hu, M., Kita, K., Kondo, Y., Li, X., Lou, S. R., Nehr, S., Shao, M., Zeng, L. M., Wahner, A., Zhang, Y. H., and Hofzumahaus, A.: Observation and modelling of OH and HO$_2$ concentrations in the Pearl River Delta 2006: a missing OH source in a VOC rich atmosphere, Atmos. Chem. Phys., 12, 1541-1569, https://doi.org/10.5194/acp-12-1541-2012, 2012.

Lu, K. D., Hofzumahaus, A., Holland, F., Bohn, B., Brauers, T., Fuchs, H., Hu, M., Häseler, R., Kita, K., Kondo, Y., Li, X., Lou, S. R., Oebel, A., Shao, M., Zeng, L. M., Wahner, A., Zhu, T., Zhang, Y. H., and Rohrer, F.: Missing OH source in a suburban environment near Beijing: observed and modelled OH and HO$_2$ concentrations in summer 2006, Atmos. Chem. Phys., 13, 1057-1080, https://doi.org/10.5194/acp-13-1057-2013, 2013.

Lu, K. D., Rohrer, F., Holland, F., Fuchs, H., Brauers, T., Oebel, A., Dlugi, R., Hu, M., Li, X., Lou, S. R., Shao, M., Zhu, T., Wahner, A., Zhang, Y. H., and Hofzumahaus, A.: Nighttime observation and chemistry of HOx in the Pearl River Delta and Beijing in summer 2006, Atmos. Chem. Phys., 14, 4979-4999, https://doi.org/10.5194/acp-14-4979-2014, 2014.

Lu, X., Hong, J., Zhang, L., Cooper, O. R., Schultz, M. G., Xu, X., Wang, T., Gao, M., Zhao, Y., and Zhang, Y.: Severe Surface Ozone Pollution in China: A Global Perspective, Environmental Science & Technology Letters, 5, 487-494, https://doi.org/10.1021/acs.estlett.8b00366, 2018.

Mebel, A. M., Lin, M. C., and Melius, C. F.: Rate Constant of the HONO + HONO → H$_2$O + NO + NO$_2$ Reaction from ab Initio MO and TST Calculations, The Journal of Physical Chemistry A, 102, 1803-1807, https://doi.org/10.1021/jp973449w, 1998.

Meng, F., Qin, M., Tang, K., Duan, J., Fang, W., Liang, S., Ye, K., Xie, P., Sun, Y., Xie, C., Ye, C., Fu, P., Liu, J., and Liu, W.: High-resolution vertical distribution and sources of HONO and NO$_2$ in the nocturnal boundary layer in urban Beijing, China, Atmos. Chem. Phys., 20, 5071-5092, https://doi.org/10.5194/acp-20-5071-2020, 2020.

Meusel, H., Kuhn, U., Reiffs, A., Mallik, C., Harder, H., Martinez, M., Schuladen, J., Bohn, B., Parchatka, U., Crowley, J. N., Fischer, H., Tomsche, L., Novelli, A., Hoffmann, T., Janssen, R. H. H., Hartogensis, O., Pikridas, M., Vrekoussis, M., Bourtsoukidis, E., Weber, B., Lelieveld, J., Williams, J., Pöschl, U., Cheng, Y., and Su, H.: Daytime formation of nitrous acid at a coastal remote site in Cyprus indicating a common ground source of atmospheric HONO and NO, Atmos. Chem. Phys., 16, 14475-14493, https://doi.org/10.5194/acp-16-14475-2016, 2016.

Michoud, V., Kukui, A., Camredon, M., Colomb, A., Borbon, A., Miet, K., Aumont, B., Beekmann, M., Durand-Jolibois, R., Perrier, S., Zapf, P., Siour, G., Ait-Helal, W., Locoge, N., Sauvage, S., Afif, C., Gros, V., Furger, M., Ancellet, G., and Doussin, J. F.: Radical budget analysis in a suburban European site during the MEGAPOLI summer field campaign, Atmos. Chem. Phys., 12, 11951-11974, https://doi.org/10.5194/acp-12-11951-2012, 2012.

Michoud, V., Colomb, A., Borbon, A., Miet, K., Beekmann, M., Camredon, M., Aumont, B., Perrier, S., Zapf, P., Siour, G., Ait-Helal, W., Afif, C., Kukui, A., Furger, M., Dupont, J. C., Haeffelin, M., and Doussin, J. F.: Study of the unknown HONO daytime source at a European suburban site during the MEGAPOLI summer and winter field campaigns, Atmos. Chem. Phys., 14, 2805-2822, https://doi.org/10.5194/acp-14-2805-2014, 2014.

Monge, M. E., D'Anna, B., Mazri, L., Giroir-Fendler, A., Ammann, M., Donaldson, D. J., and George, C.: Light changes the atmospheric reactivity of soot, Proceedings of the National Academy of Sciences, 107, 6605-6609, https://doi.org/10.1073/pnas.0908341107, 2010.

Nakashima, Y., and Kajii, Y.: Determination of nitrous acid emission factors from a gasoline vehicle using a chassis dynamometer combined with incoherent broadband cavity-enhanced absorption spectroscopy, Science of The Total Environment, 575, 287-293, https://doi.org/10.1016/j.scitotenv.2016.10.050, 2017.

Oswald, R., Behrendt, T., Ermel, M., Wu, D., Su, H., Cheng, Y., Breuninger, C., Moravek, A., Mougin, E., Delon, C., Loubet, B., Pommerening-Röser, A., Sörgel, M., Pöschl, U., Hoffmann, T., Andreae, M. O., Meixner, F. X., and Trebs, I.: HONO Emissions from Soil Bacteria as a Major Source of Atmospheric Reactive Nitrogen, Science, 341, 1233-1235, https://doi.org/10.1126/science.1242266, 2013.

Perner, D., and Platt, U.: Detection of nitrous acid in the atmosphere by differential optical absorption, Geophysical Research Letters, 6, 917-920, https://doi.org/10.1029/GL006i012p00917, 1979.

Pitts, J. N., Biermann, H. W., Winer, A. M., and Tuazon, E. C.: Spectroscopic identification and measurement of gaseous nitrous acid in dilute auto exhaust, Atmospheric Environment (1967), 18, 847-854, https://doi.org/10.1016/0004-6981(84)90270-1, 1984.

Porada, P., Tamm, A., Raggio, J., Cheng, Y., Kleidon, A., Pöschl, U., and Weber, B.: Global NO and HONO emissions of biological soil crusts estimated by a process-based non-vascular vegetation model, Biogeosciences, 16, 2003-2031, https://doi.org/10.5194/bg-16-2003-2019, 2019.

Pusede, S. E., VandenBoer, T. C., Murphy, J. G., Markovic, M. Z., Young, C. J., Veres, P. R., Roberts, J. M., Washenfelder, R. A., Brown, S. S., Ren, X., Tsai, C., Stutz, J., Brune, W. H., Browne, E. C., Wooldridge, P. J., Graham, A. R., Weber, R., Goldstein, A. H., Dusanter, S., Griffith, S. M., Stevens, P. S., Lefer, B. L., and Cohen, R. C.: An Atmospheric Constraint on the NO2 Dependence of Daytime Near-Surface Nitrous Acid (HONO), Environmental Science & Technology, 49, 12774-12781, https://doi.org/10.1021/acs.est.5b02511, 2015.

Qin, M., Xie, P., Su, H., Gu, J., Peng, F., Li, S., Zeng, L., Liu, J., Liu, W., and Zhang, Y.: An observational study of the HONO–NO2 coupling at an urban site in Guangzhou City, South China, Atmospheric Environment, 43, 5731-5742, https://doi.org/10.1016/j.atmosenv.2009.08.017, 2009.

Rappenglück, B., Lubertino, G., Alvarez, S., Golovko, J., Czader, B., and Ackermann, L.: Radical precursors and related species from traffic as observed and modeled at an urban highway junction, Journal of the Air & Waste Management Association, 63, 1270-1286, https://doi.org/10.1080/10962247.2013.822438, 2013.

Reisinger, A. R.: Observations of HNO2 in the polluted winter atmosphere: possible heterogeneous production on aerosols, Atmospheric Environment, 34, 3865-3874, https://doi.org/10.1016/S1352-2310(00)00179-5, 2000.

Rohrer, F., and Berresheim, H.: Strong correlation between levels of tropospheric hydroxyl radicals and solar ultraviolet radiation, Nature, 442, 184-187, https://doi.org/10.1038/nature04924, 2006.

Romanias, M. N., El Zein, A., and Bedjanian, Y.: Reactive uptake of HONO on aluminium oxide surface, Journal of Photochemistry and Photobiology A: Chemistry, 250, 50-57, https://doi.org/10.1016/j.jphotochem.2012.09.018, 2012.

Saliba, N. A., Yang, H., and Finlayson-Pitts, B. J.: Reaction of Gaseous Nitric Oxide with Nitric Acid on Silica Surfaces in the Presence of Water at Room Temperature, The Journal of Physical Chemistry A, 105, 10339-10346, https://doi.org/10.1021/jp012330r, 2001.

Sarwar, G., Roselle, S. J., Mathur, R., Appel, W., Dennis, R. L., and Vogel, B.: A comparison of CMAQ HONO predictions with observations from the Northeast Oxidant and Particle Study, Atmospheric Environment, 42, 5760-5770, https://doi.org/10.1016/j.atmosenv.2007.12.065, 2008.

Shao, M., Ren, X., Wang, H., Zeng, L., Zhang, Y., and Tang, X.: Quantitative relationship between production and removal of OH and HO2 radicals in urban atmosphere, Chinese Science Bulletin, 49, 2253-2258, https://doi.org/10.1360/04wb0006, 2004.

Shi, X., Ge, Y., Zheng, J., Ma, Y., Ren, X., and Zhang, Y.: Budget of nitrous acid and its impacts on atmospheric oxidative capacity at an urban site in the central Yangtze River Delta region of China, Atmospheric Environment, 238, 117725, https://doi.org/10.1016/j.atmosenv.2020.117725, 2020.

Slater, E. J., Whalley, L. K., Woodward-Massey, R., Ye, C., Lee, J. D., Squires, F., Hopkins, J. R., Dunmore, R. E., Shaw, M., Hamilton, J. F., Lewis, A. C., Crilley, L. R., Kramer, L., Bloss, W., Vu, T., Sun, Y., Xu, W., Yue, S., Ren, L., Acton, W. J. F., Hewitt, C. N., Wang, X., Fu, P., and Heard, D. E.: Elevated levels of OH observed in haze events during wintertime in central Beijing, Atmos. Chem. Phys., 20, 14847-14871, https://doi.org/10.5194/acp-20-14847-2020, 2020.

Song, L., Deng, T., and Wu, D.: Study on planetary boundary layer height in a typical haze period and different weather types over Guangzhou, Acta Scientiae Circumstantiae, 39(5), 1381-1391, http://www.cnki.net/kcms/doi/10.13671/j.hjkxxb.2019.0080.html, 2019.

Sörgel, M., Regelin, E., Bozem, H., Diesch, J. M., Drewnick, F., Fischer, H., Harder, H., Held, A., Hosaynali-Beygi, Z., Martinez, M., and Zetzsch, C.: Quantification of the unknown HONO daytime source and its relation to NO2, Atmos. Chem. Phys., 11, 10433-10447, https://doi.org/10.5194/acp-11-10433-2011, 2011a.

Sörgel, M., Trebs, I., Serafimovich, A., Moravek, A., Held, A., and Zetzsch, C.: Simultaneous HONO measurements in and above a forest canopy: influence of turbulent exchange on mixing ratio differences, Atmos. Chem. Phys., 11, 841-855, https://doi.org/10.5194/acp-11-841-2011, 2011b.

Stemmler, K., Ammann, M., Donders, C., Kleffmann, J., and George, C.: Photosensitized reduction of nitrogen dioxide on humic acid as a source of nitrous acid, Nature, 440, 195-198, https://doi.org/10.1038/nature04603, 2006.

Stutz, J., Kim, E. S., Platt, U., Bruno, P., Perrino, C., and Febo, A.: UV-visible absorption cross sections of nitrous acid, Journal of Geophysical Research: Atmospheres, 105, 14585-14592, https://doi.org/10.1029/2000JD900003, 2000.

Stutz, J., Alicke, B., and Neftel, A.: Nitrous acid formation in the urban atmosphere: Gradient measurements of NO_2 and HONO over grass in Milan, Italy, Journal of Geophysical Research: Atmospheres, 107, 8192, https://doi.org/10.1029/2001JD000390, 2002.

Stutz, J., Alicke, B., Ackermann, R., Geyer, A., Wang, S., White, A. B., Williams, E. J., Spicer, C. W., and Fast, J. D.: Relative humidity dependence of HONO chemistry in urban areas, Journal of Geophysical Research: Atmospheres, 109, https://doi.org/10.1029/2003JD004135, 2004.

Su, H.: HONO: a study to its sources and impacts from field measurements at the sub-urban areas of PRD region, Ph.D. thsis, College of Environmental Sciences and Engineering, Peking University, China, 2008.

Su, H., Cheng, Y. F., Cheng, P., Zhang, Y. H., Dong, S., Zeng, L. M., Wang, X., Slanina, J., Shao, M., and Wiedensohler, A.: Observation of nighttime nitrous acid (HONO) formation at a non-urban site during PRIDE-PRD2004 in China, Atmospheric Environment, 42, 6219-6232, https://doi.org/10.1016/j.atmosenv.2008.04.006, 2008a.

Su, H., Cheng, Y. F., Shao, M., Gao, D. F., Yu, Z. Y., Zeng, L. M., Slanina, J., Zhang, Y. H., and Wiedensohler, A.: Nitrous acid (HONO) and its daytime sources at a rural site during the 2004 PRIDE-PRD experiment in China, Journal of Geophysical Research, 113, https://doi.org/10.1029/2007JD009060, 2008b.

Su, H., Cheng, Y., Oswald, R., Behrendt, T., Trebs, I., Meixner, F. X., Andreae, M. O., Cheng, P., Zhang, Y., and Pöschl, U.: Soil Nitrite as a Source of Atmospheric HONO and OH Radicals, Science, 333, 1616-1618, https://doi.org/10.1126/science.1207687, 2011.

Tan, Z., Fuchs, H., Lu, K., Hofzumahaus, A., Bohn, B., Broch, S., Dong, H., Gomm, S., Häseler, R., He, L., Holland, F., Li, X., Liu, Y., Lu, S., Rohrer, F., Shao, M., Wang, B., Wang, M., Wu, Y., Zeng, L., Zhang, Y., Wahner, A., and Zhang, Y.: Radical chemistry at a rural site (Wangdu) in the North China Plain: observation and model calculations of OH, HO_2 and RO_2 radicals, Atmos. Chem. Phys., 17, 663-690, https://doi.org/10.5194/acp-17-663-2017, 2017.

Tan, Z., Rohrer, F., Lu, K., Ma, X., Bohn, B., Broch, S., Dong, H., Fuchs, H., Gkatzelis, G. I., Hofzumahaus, A., Holland, F., Li, X., Liu, Y., Liu, Y., Novelli, A., Shao, M., Wang, H., Wu, Y., Zeng, L., Hu, M., Kiendler-Scharr, A., Wahner, A., and Zhang, Y.: Wintertime photochemistry in Beijing: observations of ROx radical concentrations in the North China Plain during the BEST-ONE campaign, Atmos. Chem. Phys., 18, 12391-12411, https://doi.org/10.5194/acp-18-12391-2018, 2018.

Tan, Z., Lu, K., Hofzumahaus, A., Fuchs, H., Bohn, B., Holland, F., Liu, Y., Rohrer, F., Shao, M., Sun, K., Wu, Y., Zeng, L., Zhang, Y., Zou, Q., Kiendler-Scharr, A., Wahner, A., and Zhang, Y.: Experimental budgets of OH, HO2, and RO2 radicals and implications for ozone formation in the Pearl River Delta in China 2014, Atmos. Chem. Phys., 19, 7129-7150, https://doi.org/10.5194/acp-19-7129-2019, 2019.

Tang, X. Y.: The characteristics of urban air pollution in China, in Urbanization, energy, and air pollution in China: The challenges ahead, Proceedings of A Symposium, 47-54, DOI : 10.17226/11192, 2004.

Tian, Z., Yang, W., Yu, X., Zhang, M., Zhang, H., Cheng, D., Cheng, P., and Wang, B.: HONO pollution characteristics and nighttime sources during autumn in Guangzhou, China Environmental Science, 39 (05), 2000-2009, https://doi.org/10.13227/j.hjkx.201709269, 2018.

Tong, S., Hou, S., Zhang, Y., Chu, B., Liu, Y., He, H., Zhao, P., and Ge, M.: Comparisons of measured nitrous acid (HONO) concentrations in a pollution period at urban and suburban Beijing, in autumn of 2014, Science China Chemistry, 58, 1393-1402, https://doi.org/10.1007/s11426-015-5454-2, 2015.

Tong, S., Hou, S., Zhang, Y., Chu, B., Liu, Y., He, H., Zhao, P., and Ge, M.: Exploring the nitrous acid (HONO) formation mechanism in winter Beijing: direct emissions and heterogeneous production in urban and suburban areas, Faraday Discuss, 189, 213-230, https://doi.org/10.1039/C5FD00163C, 2016.

Trinh, H. T., Imanishi, K., Morikawa, T., Hagino, H., and Takenaka, N.: Gaseous nitrous acid (HONO) and nitrogen oxides (NOx) emission from gasoline and diesel vehicles under real-world driving test cycles, Journal of the Air & Waste Management Association, 67, 412-420, https://doi.org/10.1080/10962247.2016.1240726, 2017.

Tsai, C., Spolaor, M., Colosimo, S. F., Pikelnaya, O., Cheung, R., Williams, E., Gilman, J. B., Lerner, B. M., Zamora, R. J., Warneke, C., Roberts, J. M., Ahmadov, R., de Gouw, J., Bates, T., Quinn, P. K., and Stutz, J.: Nitrous acid formation in a snow-free wintertime polluted rural area, Atmos. Chem. Phys., 18, 1977-1996, https://doi.org/10.5194/acp-18-1977-2018, 2018.

VandenBoer, T. C., Brown, S. S., Murphy, J. G., Keene, W. C., Young, C. J., Pszenny, A. A. P., Kim, S., Warneke, C., de Gouw, J. A., Maben, J. R., Wagner, N. L., Riedel, T. P., Thornton, J. A., Wolfe, D. E., Dubé, W. P., Öztürk, F., Brock, C. A.,

Grossberg, N., Lefer, B., Lerner, B., Middlebrook, A. M., and Roberts, J. M.: Understanding the role of the ground surface in HONO vertical structure: High resolution vertical profiles during NACHTT-11, Journal of Geophysical Research: Atmospheres, 118, 10,155-110,171, https://doi.org/10.1002/jgrd.50721, 2013.

950 Villena, G., Kleffmann, J., Kurtenbach, R., Wiesen, P., Lissi, E., Rubio, M. A., Croxatto, G., and Rappenglück, B.: Vertical gradients of HONO, NOx and O_3 in Santiago de Chile, Atmospheric Environment, 45, 3867-3873, https://doi.org/10.1016/j.atmosenv.2011.01.073, 2011.

Vogel, B., Vogel, H., Kleffmann, J., and Kurtenbach, R.: Measured and simulated vertical profiles of nitrous acid—Part

955 II. Model simulations and indications for a photolytic source, Atmospheric Environment, 37, 2957-2966, https://doi.org/10.1016/S1352-2310(03)00243-7, 2003.

Voogt, J. A., and Oke, T. R.: Complete Urban Surface Temperatures, Journal of Applied Meteorology, 36, 1117-1132, https://doi.org/10.1175/1520-0450(1997)036<1117:CUST>2.0.CO;2, 1997.

Wall, K. J., and Harris, G. W.: Uptake of nitrogen dioxide (NO2) on acidic aqueous humic acid (HA) solutions as a

960 missing daytime nitrous acid (HONO) surface source, Journal of Atmospheric Chemistry, 74, 283-321, https://doi.org/10.1007/s10874-016-9342-8, 2017.

Wang, G., Zhang, R., Gomez, M. E., Yang, L., Levy Zamora, M., Hu, M., Lin, Y., Peng, J., Guo, S., Meng, J., Li, J., Cheng, C., Hu, T., Ren, Y., Wang, Y., Gao, J., Cao, J., An, Z., Zhou, W., Li, G., Wang, J., Tian, P., Marrero-Ortiz, W., Secrest, J., Du, Z., Zheng, J., Shang, D., Zeng, L., Shao, M., Wang, W., Huang, Y., Wang, Y., Zhu, Y., Li, Y., Hu, J., Pan, B., Cai, L.,

965 Cheng, Y., Ji, Y., Zhang, F., Rosenfeld, D., Liss, P. S., Duce, R. A., Kolb, C. E., and Molina, M. J.: Persistent sulfate formation from London Fog to Chinese haze, Proceedings of the National Academy of Sciences, 113, 13630-13635, https://doi.org/10.1073/pnas.1616540113, 2016.

Wang, G., Ma, S., Niu, X., Chen, X., Liu, F., Li, X., Li, L., Shi, G., and Wu, Z.: Barrierless HONO and HOS(O)2-NO2 Formation via NH3-Promoted Oxidation of SO2 by NO2, The Journal of Physical Chemistry A, 125, 2666-2672,

970 https://doi.org/10.1021/acs.jpca.1c00539, 2021a.

Wang, J., Zhang, X., Guo, J., Wang, Z., and Zhang, M.: Observation of nitrous acid (HONO) in Beijing, China: Seasonal variation, nocturnal formation and daytime budget, Science of The Total Environment, 587-588, 350-359, https://doi.org/10.1016/j.scitotenv.2017.02.159, 2017a.

Wang, S., Zhou, R., Zhao, H., Wang, Z., Chen, L., and Zhou, B.: Long-term observation of atmospheric nitrous acid

975 (HONO) and its implication to local NO_2 levels in Shanghai, China, Atmospheric Environment, 77, 718-724, https://doi.org/10.1016/j.atmosenv.2013.05.071, 2013.

Wang, T., Wei, X. L., Ding, A. J., Poon, C. N., Lam, K. S., Li, Y. S., Chan, L. Y., and Anson, M.: Increasing surface ozone concentrations in the background atmosphere of Southern China, 1994–2007, Atmos. Chem. Phys., 9, 6217-6227, https://doi.org/10.5194/acp-9-6217-2009, 2009.

980 Wang, T., Xue, L., Brimblecombe, P., Lam, Y. F., Li, L., and Zhang, L.: Ozone pollution in China: A review of concentrations, meteorological influences, chemical precursors, and effects, Science of The Total Environment, 575, 1582-1596, https://doi.org/10.1016/j.scitotenv.2016.10.081, 2017b.

Wang, Y., Fu, X., Wu, D., Wang, M., Lu, K., Mu, Y., Liu, Z., Zhang, Y., and Wang, T.: Agricultural Fertilization Aggravates Air Pollution by Stimulating Soil Nitrous Acid Emissions at High Soil Moisture, Environmental Science &

985 Technology, 55, 14556-14566, https://doi.org/10.1021/acs.est.1c04134, 2021b.

Weber, B., Wu, D., Tamm, A., Ruckteschler, N., Rodriguez-Caballero, E., Steinkamp, J., Meusel, H., Elbert, W., Behrendt, T., Sorgel, M., Cheng, Y., Crutzen, P. J., Su, H., and Poschl, U.: Biological soil crusts accelerate the nitrogen cycle through large NO and HONO emissions in drylands, Proceedings of the National Academy of Sciences, 112, 15384-15389, https://doi.org/10.1073/pnas.1515818112, 2015.

990 Wong, K. W., Oh, H. J., Lefer, B. L., Rappenglück, B., and Stutz, J.: Vertical profiles of nitrous acid in the nocturnal urban atmosphere of Houston, TX, Atmos. Chem. Phys., 11, 3595-3609, https://doi.org/10.5194/acp-11-3595-2011, 2011.

Wong, K. W., Tsai, C., Lefer, B., Haman, C., Grossberg, N., Brune, W. H., Ren, X., Luke, W., and Stutz, J.: Daytime HONO vertical gradients during SHARP 2009 in Houston, TX, Atmos. Chem. Phys., 12, 635-652, https://doi.org/10.5194/acp-12-635-2012, 2012.

995 Wong, K. W., Tsai, C., Lefer, B., Grossberg, N., and Stutz, J.: Modeling of daytime HONO vertical gradients during SHARP 2009, Atmos. Chem. Phys., 13, 3587-3601, https://doi.org/10.5194/acp-13-3587-2013, 2013.

Wu, C., Wu, D., and Yu, J. Z.: Quantifying black carbon light absorption enhancement with a novel statistical approach, Atmos. Chem. Phys., 18, 289-309, https://doi.org/10.5194/acp-18-289-2018, 2018.

1000 Wu, D., Horn, M. A., Behrendt, T., Muller, S., Li, J., Cole, J. A., Xie, B., Ju, X., Li, G., Ermel, M., Oswald, R., Frohlich-Nowoisky, J., Hoor, P., Hu, C., Liu, M., Andreae, M. O., Poschl, U., Cheng, Y., Su, H., Trebs, I., Weber, B., and Sorgel, M.: Soil HONO emissions at high moisture content are driven by microbial nitrate reduction to nitrite: tackling the HONO puzzle, ISME J, 13, 1688-1699, https://doi.org/10.1038/s41396-019-0379-y, 2019.

Wu, Y., Li, S., and Yu, S.: Monitoring urban expansion and its effects on land use and land cover changes in Guangzhou city, China, Environmental Monitoring and Assessment, 188, 54, https://doi.org/10.1007/s10661-015-5069-2, 2015.

1005 Xia, D., Zhang, X., Chen, J., Tong, S., Xie, H.-b., Wang, Z., Xu, T., Ge, M., and Allen, D. T.: Heterogeneous Formation of HONO Catalyzed by CO2, Environmental Science & Technology, 55, 12215-12222, https://doi.org/10.1021/acs.est.1c02706, 2021.

Xu, W., Kuang, Y., Zhao, C., Tao, J., Zhao, G., Bian, Y., Yang, W., Yu, Y., Shen, C., Liang, L., Zhang, G., Lin, W., and Xu, X.: NH3-promoted hydrolysis of NO2 induces explosive growth in HONO, Atmos. Chem. Phys., 19, 10557-10570, 1010 https://doi.org/10.5194/acp-19-10557-2019, 2019.

Xu, Z., Wang, T., Xue, L. K., Louie, P. K. K., Luk, C. W. Y., Gao, J., Wang, S. L., Chai, F. H., and Wang, W. X.: Evaluating the uncertainties of thermal catalytic conversion in measuring atmospheric nitrogen dioxide at four differently polluted sites in China, Atmospheric Environment, 76, 221-226, https://doi.org/10.1016/j.atmosenv.2012.09.043, 2013.

Xu, Z., Wang, T., Wu, J., Xue, L., Chan, J., Zha, Q., Zhou, S., Louie, P. K. K., and Luk, C. W. Y.: Nitrous acid (HONO) 1015 in a polluted subtropical atmosphere: Seasonal variability, direct vehicle emissions and heterogeneous production at ground surface, Atmospheric Environment, 106, 100-109, https://doi.org/10.1016/j.atmosenv.2015.01.061, 2015.

Xue, C., Zhang, C., Ye, C., Liu, P., Catoire, V., Krysztofiak, G., Chen, H., Ren, Y., Zhao, X., Wang, J., Zhang, F., Zhang, C., Zhang, J., An, J., Wang, T., Chen, J., Kleffmann, J., Mellouki, A., and Mu, Y.: HONO Budget and Its Role in Nitrate Formation in the Rural North China Plain, Environ Sci Technol, 54, 11048-11057, https://doi.org/10.1021/acs.est.0c01832, 1020 2020.

Xue, L., Gu, R., Wang, T., Wang, X., Saunders, S., Blake, D., Louie, P. K. K., Luk, C. W. Y., Simpson, I., Xu, Z., Wang, Z., Gao, Y., Lee, S., Mellouki, A., and Wang, W.: Oxidative capacity and radical chemistry in the polluted atmosphere of Hong Kong and Pearl River Delta region: analysis of a severe photochemical smog episode, Atmos. Chem. Phys., 16, 9891-9903, https://doi.org/10.5194/acp-16-9891-2016, 2016.

1025 Xue, L. K., Wang, T., Gao, J., Ding, A. J., Zhou, X. H., Blake, D. R., Wang, X. F., Saunders, S. M., Fan, S. J., Zuo, H. C., Zhang, Q. Z., and Wang, W. X.: Ground-level ozone in four Chinese cities: precursors, regional transport and heterogeneous processes, Atmos. Chem. Phys., 14, 13175-13188, https://doi.org/10.5194/acp-14-13175-2014, 2014.

Yabushita, A., Enami, S., Sakamoto, Y., Kawasaki, M., Hoffmann, M. R., and Colussi, A. J.: Anion-Catalyzed Dissolution of NO2 on Aqueous Microdroplets, The Journal of Physical Chemistry A, 113, 4844-4848, 1030 https://doi.org/10.1021/jp900685f, 2009.

Yang, Q.: Observations and sources analysis of gaseous nitrous acid — A case study in Beijing and Pearl River Delta area, Ph.D. thsis, College of Environmental Sciences and Engineering, Peking University, China, 2014.

Yang, Q., Su, H., Li, X., Cheng, Y., Lu, K., Cheng, P., Gu, J., Guo, S., Hu, M., Zeng, L., Zhu, T., and Zhang, Y.: Daytime HONO formation in the suburban area of the megacity Beijing, China, Science China Chemistry, 57, 1032-1042, 1035 https://doi.org/10.1007/s11426-013-5044-0, 2014.

Yang, W., Cheng, P., Tian, Z., Zhang, H., Zhang, M., and Wang, B.: Study on HONO pollution characteristics and daytime unknown sources during summer and autumn in Guangzhou, China., China Environmental Science, 37 (006), 2029-2039, DOI: 10.3969/j.issn.1000-6923.2017.06.005, 2017a.

Yang, W., You, D., Li, C., Han, C., Tang, N., Yang, H., and Xue, X.: Photolysis of Nitroaromatic Compounds under 1040 Sunlight: A Possible Daytime Photochemical Source of Nitrous Acid?, Environmental Science & Technology Letters, 8, 747-752, https://doi.org/10.1021/acs.estlett.1c00614, 2021a.

Yang, Y., Shao, M., Keßel, S., Li, Y., Lu, K., Lu, S., Williams, J., Zhang, Y., Zeng, L., Nölscher, A. C., Wu, Y., Wang, X., and Zheng, J.: How the OH reactivity affects the ozone production efficiency: case studies in Beijing and Heshan, China, Atmos. Chem. Phys., 17, 7127-7142, https://doi.org/10.5194/acp-17-7127-2017, 2017b.

1045 Yang, Y., Li, X., Zu, K., Lian, C., Chen, S., Dong, H., Feng, M., Liu, H., Liu, J., Lu, K., Lu, S., Ma, X., Song, D., Wang, W., Yang, S., Yang, X., Yu, X., Zhu, Y., Zeng, L., Tan, Q., and Zhang, Y.: Elucidating the effect of HONO on O_3 pollution by

a case study in southwest China, Science of The Total Environment, 756, 144127, https://doi.org/10.1016/j.scitotenv.2020.144127, 2021b.

Ye, C., Gao, H., Zhang, N., and Zhou, X.: Photolysis of Nitric Acid and Nitrate on Natural and Artificial Surfaces, Environ Sci Technol, 50, 3530-3536, https://doi.org/10.1021/acs.est.5b05032, 2016.

Ye, C., Zhang, N., Gao, H., and Zhou, X.: Photolysis of Particulate Nitrate as a Source of HONO and NOx, Environmental Science & Technology, 51, 6849-6856, https://doi.org/10.1021/acs.est.7b00387, 2017.

Yu, Y., Galle, B., Panday, A., Hodson, E., Prinn, R., and Wang, S.: Observations of high rates of NO2/HONO conversion in the nocturnal atmospheric boundary layer in Kathmandu, Nepal, Atmos. Chem. Phys., 9, 6401-6415, https://doi.org/10.5194/acp-9-6401-2009, 2009.

Yue, D. L., Hu, M., Wu, Z. J., Guo, S., Wen, M. T., Nowak, A., Wehner, B., Wiedensohler, A., Takegawa, N., Kondo, Y., Wang, X. S., Li, Y. P., Zeng, L. M., and Zhang, Y. H.: Variation of particle number size distributions and chemical compositions at the urban and downwind regional sites in the Pearl River Delta during summertime pollution episodes, Atmos. Chem. Phys., 10, 9431-9439, https://doi.org/10.5194/acp-10-9431-2010, 2010.

Yue, D. L., Zhong, L., Shen, J., Zhang, T., Zhou, Y., Zeng, L., and Dong, H.: Pollution properties of atmospheric HNO_2 and its effect on OH radical formation in the PRD region in autumn, Environmental Science & Technology, 162-166, DOI: 10.3969/j.issn.1003-6504.2016.02.030, 2016.

Yun, H., Wang, Z., Zha, Q., Wang, W., Xue, L., Zhang, L., Li, Q., Cui, L., Lee, S., Poon, S. C. N., and Wang, T.: Nitrous acid in a street canyon environment: Sources and contributions to local oxidation capacity, Atmospheric Environment, 167, 223-234, https://doi.org/10.1016/j.atmosenv.2017.08.018, 2017.

Yun, H.: Reactive nitrogen ocides (HONO, N_2O_5 and $ClNO_2$) in different atmospheric environment in China: concentrations formation and the impact on atmospheric oxidation capacity, Ph.D. thsis. Department of Civil and Environmental Engineering, The Hong Kong Polytechnic University, China, 2018.

Zha, Q., Xue, L., Wang, T., Xu, Z., Yeung, C., Louie, P. K. K., and Luk, C. W. Y.: Large conversion rates of NO_2 to HNO_2 observed in air masses from the South China Sea: Evidence of strong production at sea surface?, Geophysical Research Letters, 41, 7710-7715, https://doi.org/10.1002/2014GL061429, 2014.

Zhang, B., and Tao, F.-M.: Direct homogeneous nucleation of NO_2, H_2O, and NH_3 for the production of ammonium nitrate particles and HONO gas, Chemical Physics Letters, 489, 143-147, https://doi.org/10.1016/j.cplett.2010.02.059, 2010.

Zhang, N., Zhou, X., Shepson, P. B., Gao, H., Alaghmand, M., and Stirm, B.: Aircraft measurement of HONO vertical profiles over a forested region, Geophysical Research Letters, 36, https://doi.org/10.1029/2009GL038999, 2009.

Zhang, S., Sarwar, G., Xing, J., Chu, B., Xue, C., Sarav, A., Ding, D., Zheng, H., Mu, Y., Duan, F., Ma, T., and He, H.: Improving the representation of HONO chemistry in CMAQ and examining its impact on haze over China, Atmos. Chem. Phys., 21, 15809-15826, https://doi.org/10.5194/acp-21-15809-2021, 2021.

Zhang, W., Tong, S., Ge, M., An, J., Shi, Z., Hou, S., Xia, K., Qu, Y., Zhang, H., Chu, B., Sun, Y., and He, H.: Variations and sources of nitrous acid (HONO) during a severe pollution episode in Beijing in winter 2016, Science of The Total Environment, 648, 253-262, https://doi.org/10.1016/j.scitotenv.2018.08.133, 2019.

Zhao, X., Shi, X., Ma, X., Wang, J., Xu, F., Zhang, Q., Li, Y., Teng, Z., Han, Y., Wang, Q., and Wang, W.: Simulation Verification of Barrierless HONO Formation from the Oxidation Reaction System of NO, Cl, and Water in the Atmosphere, Environmental Science & Technology, 55, 7850-7857, https://doi.org/10.1021/acs.est.1c01773, 2021.

Zheng, J., Zhong, L., Wang, T., Louie, P. K. K., and Li, Z.: Ground-level ozone in the Pearl River Delta region: Analysis of data from a recently established regional air quality monitoring network, Atmospheric Environment, 44, 814-823, https://doi.org/10.1016/j.atmosenv.2009.11.032, 2010.

Zheng, J., Shi, X., Ma, Y., Ren, X., Jabbour, H., Diao, Y., Wang, W., Ge, Y., Zhang, Y., and Zhu, W.: Contribution of nitrous acid to the atmospheric oxidation capacity in an industrial zone in the Yangtze River Delta region of China, Atmos. Chem. Phys., 20, 5457-5475, https://doi.org/10.5194/acp-20-5457-2020, 2020.

Zhong, L., Louie, P. K. K., Zheng, J., Yuan, Z., Yue, D., Ho, J. W. K., and Lau, A. K. H.: Science–policy interplay: Air quality management in the Pearl River Delta region and Hong Kong, Atmospheric Environment, 76, 3-10, https://doi.org/10.1016/j.atmosenv.2013.03.012, 2013.

Zhou, X., Civerolo, K., Dai, H., Huang, G., Schwab, J., and Demerjian, K.: Summertime nitrous acid chemistry in the atmospheric boundary layer at a rural site in New York State, Journal of Geophysical Research: Atmospheres, 107, ACH 13-11-ACH 13-11, https://doi.org/10.1029/2001JD001539, 2002a.

Zhou, X., He, Y., Huang, G., Thornberry, T. D., Carroll, M. A., and Bertman, S. B.: Photochemical production of nitrous acid on glass sample manifold surface, Geophysical Research Letters, 29, 26-21-26-24, https://doi.org/10.1029/2002GL015080, 2002b.

1100 Zhou, X., Gao, H., He, Y., Huang, G., Bertman, S. B., Civerolo, K., and Schwab, J.: Nitric acid photolysis on surfaces in low-NOx environments: Significant atmospheric implications, Geophysical Research Letters, 30, https://doi.org/10.1029/2003GL018620, 2003.

Zhou, X., Huang, G., Civerolo, K., Roychowdhury, U., and Demerjian, K. L.: Summertime observations of HONO, HCHO, and O3 at the summit of Whiteface Mountain, New York, Journal of Geophysical Research: Atmospheres, 112,
1105 https://doi.org/10.1029/2006JD007256, 2007.

Zhou, X., Zhang, N., TerAvest, M., Tang, D., Hou, J., Bertman, S., Alaghmand, M., Shepson, P. B., Carroll, M. A., Griffith, S., Dusanter, S., and Stevens, P. S.: Nitric acid photolysis on forest canopy surface as a source for tropospheric nitrous acid, Nature Geoscience, 4, 440-443, https://doi.org/10.1038/ngeo1164, 2011.

1110

Supplement of

Budget of nitrous acid (HONO) at an urban site in the fall season of Guangzhou, China

Yihang Yu[1,2], Peng Cheng[1,2,5,*], Huirong Li[1,2], Wenda Yang[1,2], Baobin Han[1,2], Wei Song[3], Weiwei Hu[3], Xinming Wang[3], Bin Yuan[4,5], Min Shao[4,5], Zhijiong Huang[4], Zhen Li[4], Junyu Zheng[4,5], Haichao Wang[6] and Xiaofang Yu[1,2]

[1]Institute of Mass Spectrometry and Atmospheric Environment, Jinan University, Guangzhou 510632, China
[2]Guangdong Provincial Engineering Research Center for Online Source Apportionment System of Air Pollution, Guangzhou 510632, China(Stutz et al., 2004)
[3]State Key Laboratory of Organic Geochemistry, Guangzhou Institute of Geochemistry, Chinese Academy of Sciences, Guangzhou 510640, China
[4]Institute for Environmental and Climate Research, Jinan University, Guangzhou 511443, China
[5]Guangdong-Hongkong-Macau Joint Laboratory of Collaborative Innovation for Environmental Quality, Guangzhou 511443, China
[6]School of Atmospheric Sciences, Sun Yat-Sen University, Zhuhai, China

Correspondence to: Peng Cheng (chengp@jnu.edu.cn)

The introduction of the custom-built LOPAP

20   The LOPAP instrument was first developed by Heland et al. (2001), which is based on wet chemical sampling and photometric detection. Ambient air is sampled into an external sampling unit consisting of two similar stripping coils in series. Almost all the HONO and a small fraction of interfering substances (PAN, HNO_3, NO_2, etc.) are absorbed in solution in the first stripping coil, while in the second stripping coil only the interfering species are absorbed. To minimize the potential interferences, we assume the interferences absorbed in the first and the second coil are the same, so the real HONO concentration in the

25   atmosphere is determined by subtracting the measured signal of the second coil from the measured signal of the first coil. The absorption solution R1 is a mixture reagent of 1 L hydrochloric acid (HCl) (37% volume fraction) and 100 g sulfanilamide dissolved in 9 L pure water. The dye solution R2, 2 g n-(1-naphtyl)-ethylendiamine-dihydrchloride (NEDA) dissolved in 10 L pure water, is then reacted with the absorption solution from two stripping coils pumped by a peristaltic pump to form colored azo dye. The light-absorbing colored azo dye is then pumped through a debubbler by the peristaltic pump and flows into the

30   detection unit, which consists of two liquid waveguide capillary cells (World Precision Instrument, LWCC), one LED light source (Ocean Optics), two miniature spectrometers (Ocean Optics, Maya2000Pro) and several optical fibers. To correct for the small zero-drifts in the instrument's baseline, the zero measurements were conducted every 12 h by introducing zero air (highly pure nitrogen). During the instrument's operation, the instrument calibration was performed every week using the standard sodium nitrite ($NaNO_2$) solution (with the concentrations of 1–20 ppb, corresponding to atmospheric HONO mixing

35   ratios of 0.245–4.9 ppbv).

Detection limit is defined as 3σ of HONO concentration measured in zero air measurement. The detection limit of 5 pptv for this campaign was determined by zero air measurement. The precision (2σ) of the custom-build LOPAP is defined in this work as the minimum detectable change of a measured signal (Villena et al., 2011) and amounts to approximately 1.0% of 10 ppb

40   nitrite concentrations (median value of observed ambient HONO concentrations). This 5 pptv also serves as the precision of the instrument. Time response resolution is defined as the time interval between HONO signal decreases from 90% of the signal when start zero air running to 10% higher than the zero signal. It also relates to the liquid flow. The determined time response resolution during the campaign is about 15 4 min considering the air flow of 1 L min^{-1} and liquid flow of 0.4 mL min^{-1}. Measurement error is the sum of statistic error and systematic error. Statistic error is defined as 1σ of HONO signal in

45   zero air measurement. Systematic error is coming from the uncertainties of air flow rate, liquid flow rate and calibration factor, and is about 8% of measured HONO by applying "Gaussian Error Propagation" method (Trebs et al., 2004). The instrument parameters are listed in Table S1.

A commercial LOPAP (QUMA, Germany) operated by the Guangzhou Institute of Geochemistry Chinese Academy of

50   Sciences (GIGCAS) also measured HONO during the observation. Unfortunately, only less than 10 days data were obtained by the commercial LOPAP due to malfunction. Our custom-built LOPAP was validated against the commercial LOPAP

instrument with good agreement (R^2 = 0.910) (see Fig. S2), which further demonstrated the reliability of our instrument.

The evaluation of the interferences caused by other NO_y species on NO_2 measurement using molybdenum converter

55   Our site is a typical urban site with heavy traffic emissions, as indicated by high concentrations of NO and NOx. Meanwhile, the average concentration of HONO, gaseous HNO_3 and particulate nitrate during the campaign were 0.74 ± 0.70 ppbv, 2.1 ± 2.0 ppbv and 4.2 ± 5.8 μg m^{-3}, respectively. PAN was not measured and is estimated around 0.84 ppbv based on earlier data at Guangzhou (Wang et al., 2015a) and the other NO_y species can be ignored. Based on these, we roughly estimate the relative interferences of NOz (NOy-NOx) to NO_2 to be around 10%.

60
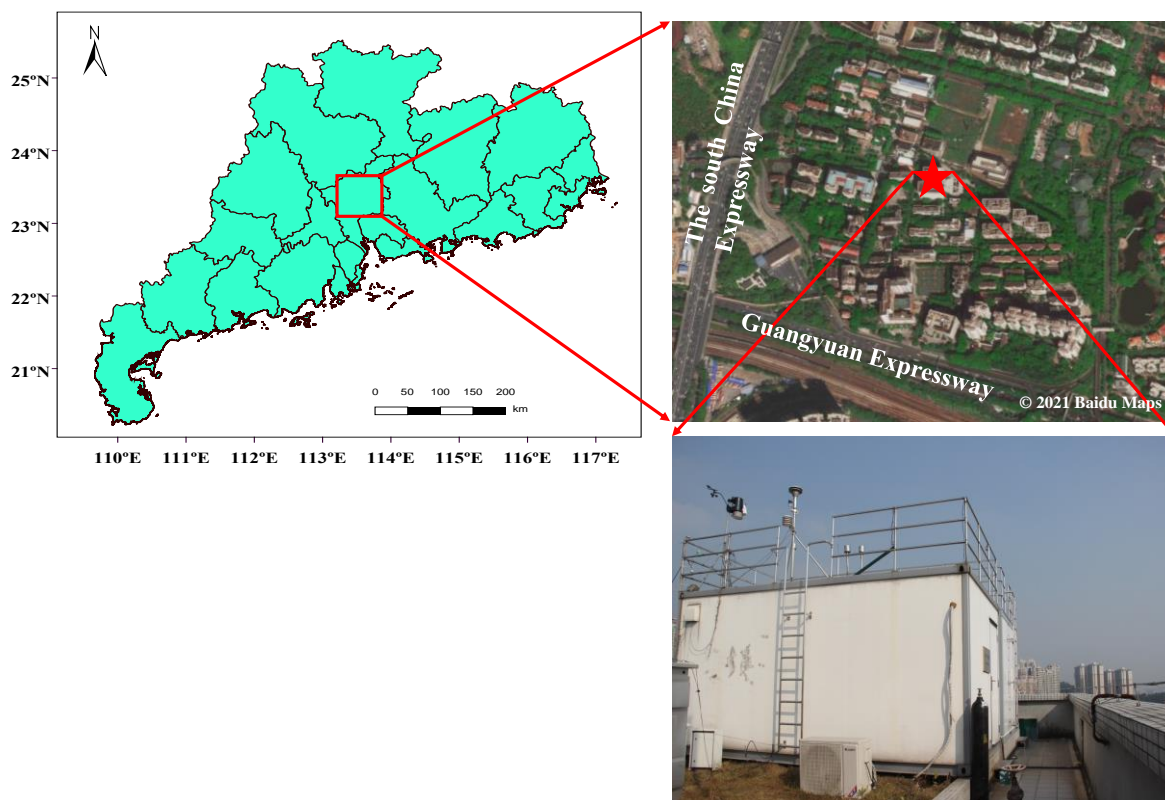
65   **Figure S1. Schematic map of the measurement site in Guangzhou. The red star represents specimen building of the Guangzhou Institute of Geochemistry, Chinese Academy of Sciences (GIGCAS).**
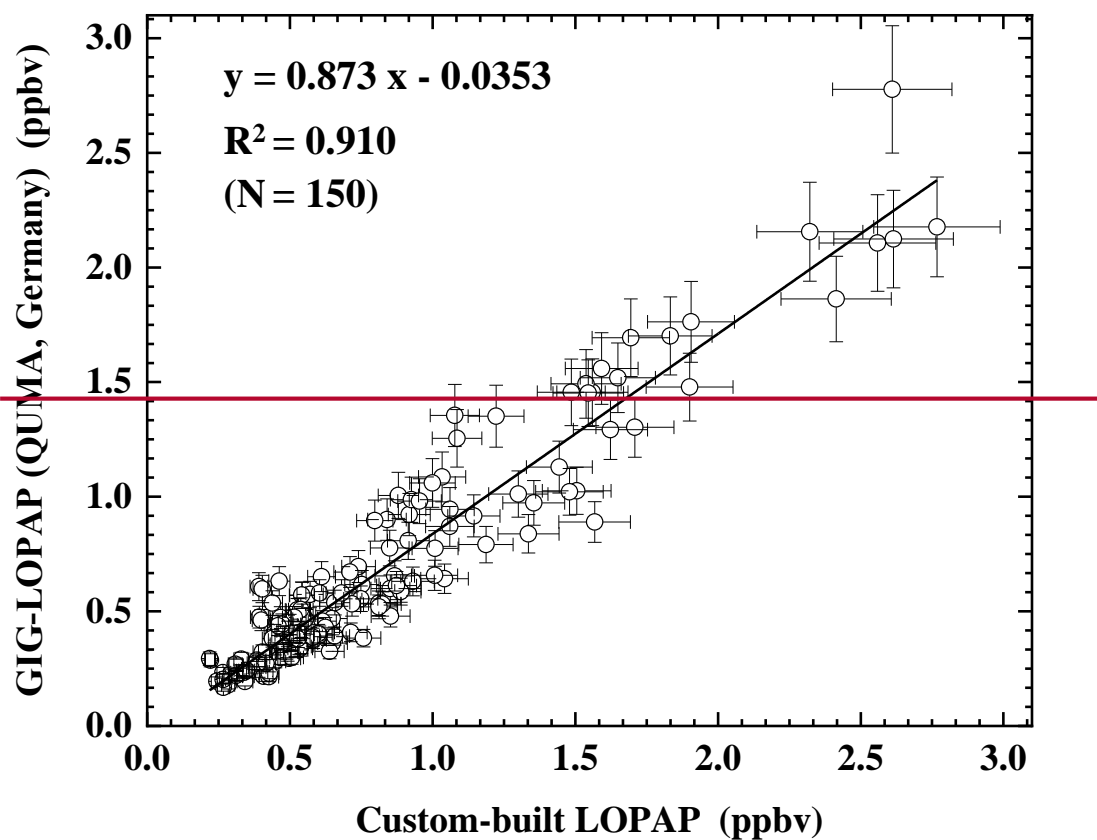
Figure S2. Intercomparison between the custom-built LOPAP with the commercial LOPAP (QUMA, Germany). The linear fitting line has an intercept of A = −0.035 ± 0.022, a slope of B = 0.873 ± 0.023 and R^2 = 0.910 (N = 150). The error bars represent the uncertainties of our custom-built LOPAP (8%) and commercial LOPAP data (QUMA, Germany) (10%). The data from October 15-18 and November 1-6, 2018 was used for comparison.

70
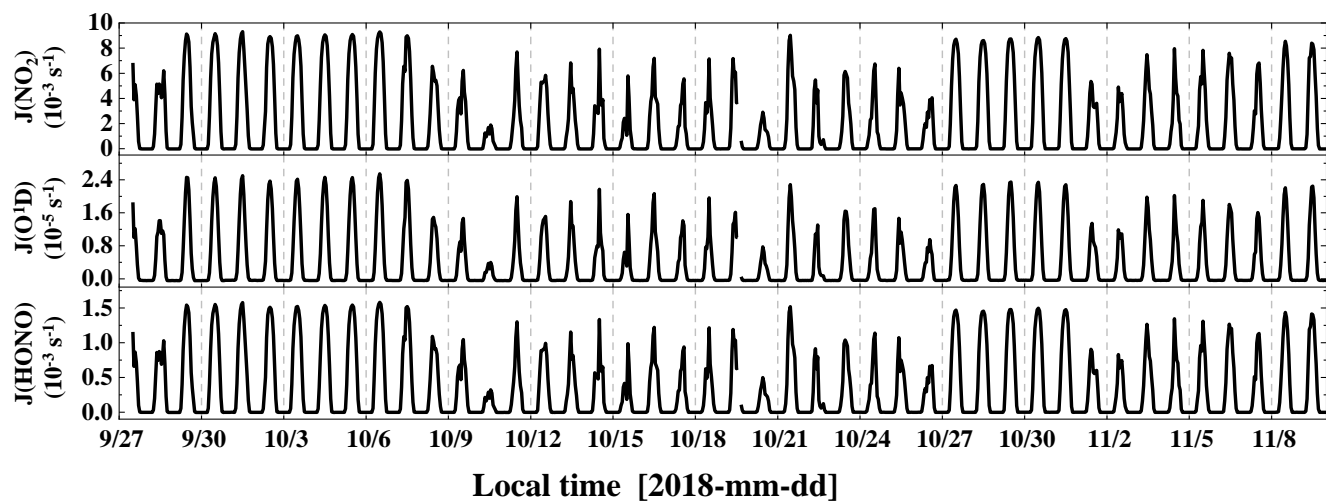
Figure S3. Temporal variations of photolysis rates J(HONO), J(O^{1}D) and J(NO$_2$) during the observation period.
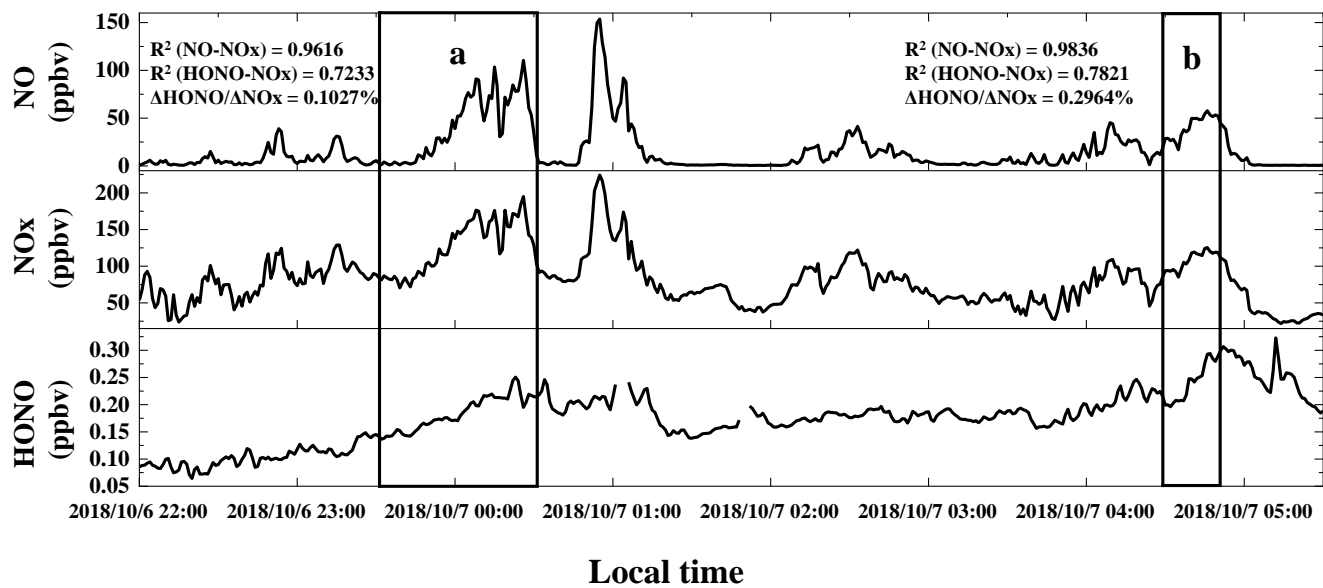
85

Figure S4. Temporal variations of nocturnal HONO, NOx and NO on October 6–7, 2018. The HONO emission factors were obtained according to the data in the black frames a and b.
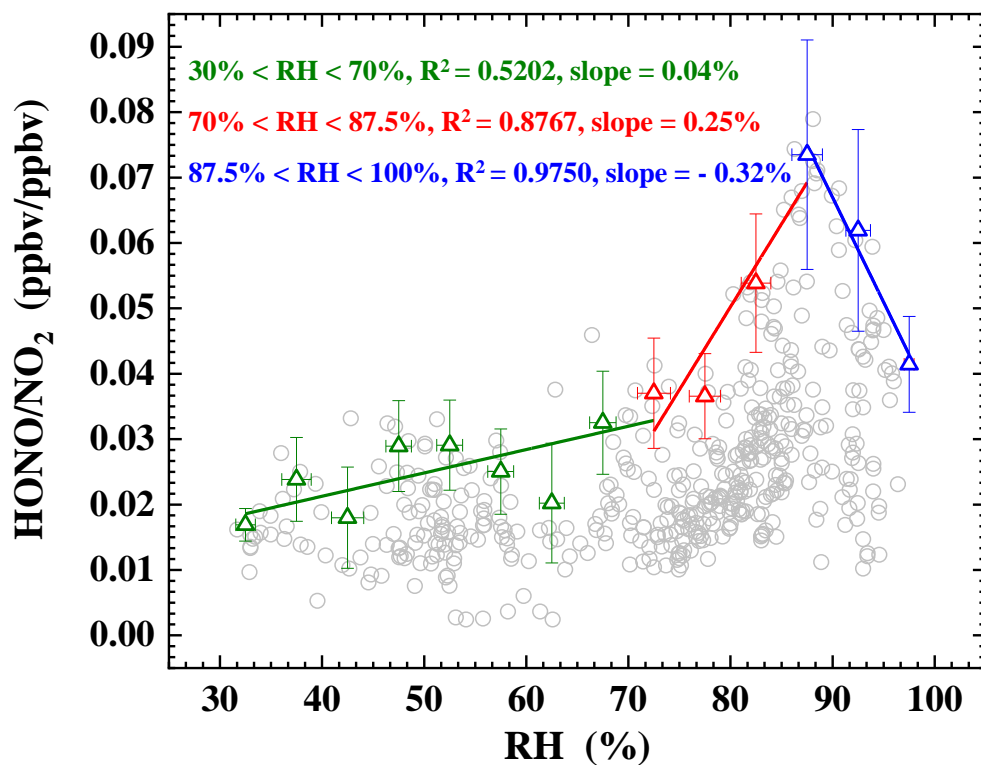
90   **Figure S5. Scatter plot of HONO/NO₂ ratio against RH during nighttime from 18:00 to 6:00. Triangles are the average of top-5 HONO/NO₂ values in each 5% RH interval.**
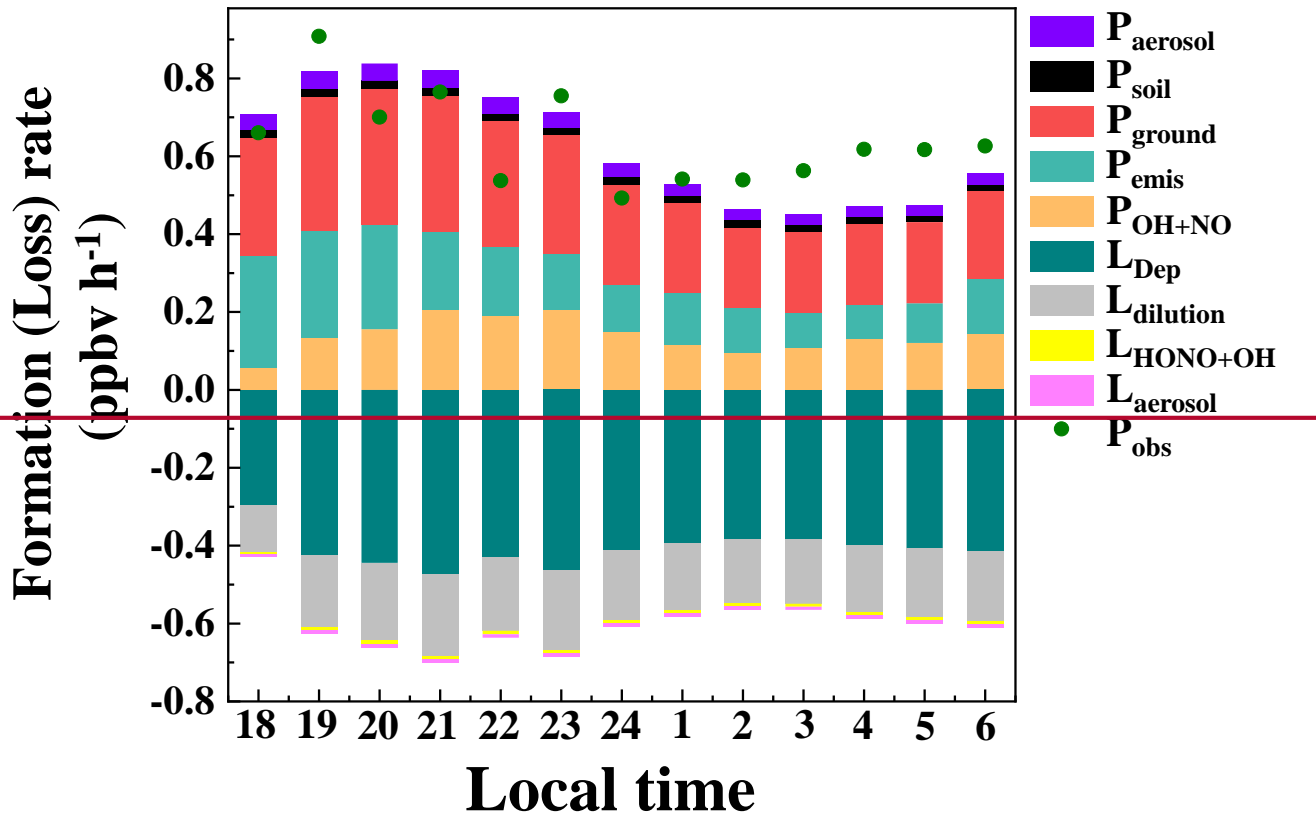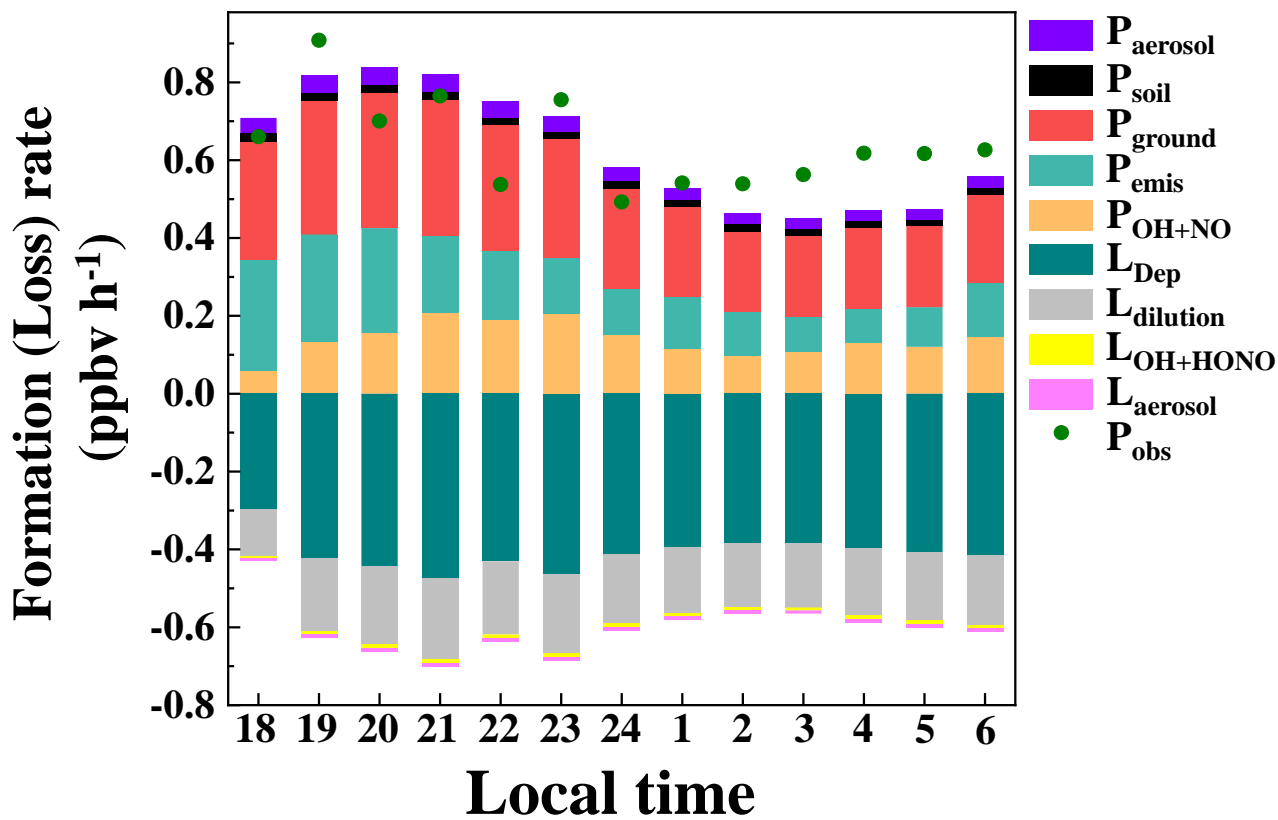
95 **Figure S6. Nighttime HONO budget in Guangzhou during the observation period.**

Table S1. The parameters of the custom-built LOPAP.

Parameters	Values
Air flow	1 L min^{-1}
Liquid flow	0.4 mL min^{-1}
Length of LWCC	100 cm
Detection limit	5 pptv
Detection range	5 pptv–10 ppbv
Time response ~~resolution~~	4~~15~~ min
Uncertainty	8%

100 **Table S2. Emission factors (ΔHONO/ΔNOx) and other information in 11 fresh plumes.**

Starting time	Duration (min)	R^2 (NO-NOx)	R^2 (HONO-NOx)	ΔNO/ΔNOx	HONO/NOx	ΔHONO/ΔNOx
2018/10/6 23:29	62	0.9616	0.7233	0.90	0.002	0.001
2018/10/7 4:29	22	0.9836	0.7821	0.97	0.002	0.003
2018/10/7 20:44	34	0.9559	0.7054	0.88	0.011	0.010
2018/10/7 22:49	22	0.9904	0.8051	1.05	0.013	0.008
2018/10/20 0:33	24	0.9621	0.7826	0.96	0.020	0.007
2018/10/21 6:28	40	0.9959	0.9403	0.89	0.021	0.014
2018/10/25 6:55	20	0.9615	0.7291	1.04	0.024	0.014
2018/11/4 19:04	22	0.9761	0.8148	1.05	0.022	0.011
2018/11/4 22:01	78	0.9892	0.7684	1.02	0.016	0.007
2018/11/6 7:31	29	0.9835	0.7902	1.03	0.029	0.009
2018/11/7 4:56	30	0.9750	0.7007	0.93	0.027	0.015

Table S3. The overview of percentage of nighttime primary emissions of HONO from urban sites in China.

Location	Date	Nighttime NOx (ppbv)	[HONO]$_{emis}$/[HONO] (%)	Emission ratio HONO/NOx (%)	Reference
Guangzhou	Oct 2015	57.9	15.1	0.65	1
Guangzhou	Sep–Nov 2018	47.7	47	0.9	2
Shanghai	May 2016	–	12.5	0.65	3
Changzhou	Apr 2017	–	31.4	0.69	4
Zhengzhou	Jan 2019	41	17[a]	0.65	5
		68.7	16[b]		
		107.3	16[c]		
Ji'nan	Nov 2013–Jan 2014	–	42	0.58	6
Ji'nan	Sep–Nov 2015	38	18	0.53	7
	Dec 2015–Feb 2016	78.5	21		
	Mar–May 2016	47.3	12		
	Jun–Aug 2016	29.1	15		
Beijing	Jan–Feb 2007	–	20.59	0.65	8
	Aug 2007	–	11.68		
Beijing	Oct–Nov 2014	94.5	39.6	0.65	9
Beijing	Dec 2015	–	48.8	0.8	10
Beijing	Dec 2015	–	52[b]	1.3	11
		–	40[c]		
Beijing	Dec 2016	–	29.3	0.78	12
Beijing	Aug–Sep 2018	–	17.6	0.8	13
Beijing	May–Jul 2018	–	14.21	0.78	14
	Nov 2018–Jan 2019	–	30.79		

[a]: clean; [b]: polluted; [c]: severely polluted. Reference: 1: Tian et al. (2018); 2: This work; 3: Cui et al. (2018); 4: Shi et al. (2020); 5: Hao et al. (2020); 6: Wang et al. (2015b); 7: Li et al. (2018); 8: Spataro et al. (2013); 9: Tong et al. (2015); 10: Tong et al. (2016); 11: Zhang et al. (2019); 12: Meng et al. (2020); 13: Jia et al. (2020); 14: Liu et al. (2021).

105

Table S4. The OH concentration is assumed of 0.5×10^6 molecules cm^{-3}. The integrated P^{net}_{OH+NO} of homogeneous reaction of NO + OH from 18:00 to 6:00.

OH/molecules cm^{-3}	Integrated P^{net}_{OH+NO}/ppbv	Measured HONO/ppbv
1×10^5	0.32	
5×10^5	1.62	0.26
1×10^6	3.24	

110

Table S5. Parameterisations of HONO production and loss mechanisms.

Mechanism	HONO formation/loss reactions	Parameterisation			Reference
		Median	Lower	Upper	
Primary emission		P_{emis} = 0.16 ppbv h^{-1}	Emission source inventory 1	Emission source inventory 2	1
NO + OH	NO + OH → HONO	OH = 0.5 × 10^6 cm^{-3}	1.0 × 10^5 cm^{-3}	1.0 × 10^6 cm^{-3}	2
NO$_2$ on aerosol	NO$_2$ + aerosol → HONO	$\gamma_{NO_2 \rightarrow aerosol}$ = 4 × 10^{-6}	2 × 10^{-7}	1 × 10^{-5}	3, 4, 5
NO$_2$ on ground	NO$_2$ + ground → HONO	$\gamma_{NO_2 \rightarrow ground}$ = 4 × 10^{-6}	2 × 10^{-7}	1 × 10^{-5}	3, 4, 5
Soil emission		water content: 35%–45%	45%–55%	25%–35%	6, 7, 8
Deposition		V_d = 2.5 cm s^{-1}	0.077 cm s^{-1}	3 cm s^{-1}	9, 10, 11,12
Vertical transport		$k_{(dilution)}$ = 0.23 h^{-1}	0.1 h^{-1}	0.44 h^{-1}	13, 14, 15
HONO on aerosol		$\gamma_{HONO \rightarrow aerosol}$ = 4×10^{-5}	3 × 10^{-7}	5 × 10^{-4}	16, 17, 18
HONO + OH	HONO + OH → NO$_2$ + H$_2$O	OH = 0.5 × 10^6 cm^{-3}	1.0 × 10^5 cm^{-3}	1.0 × 10^6 cm^{-3}	2

Emission source inventory 1 denotes the 2017 NOx emission source inventory of Guangzhou city; Emission source inventory 2 denotes the 2017 NOx emission source inventory of the 3 km × 3 km grid cell centred on the Guangzhou Institute of Geochemistry. Reference: 1: Huang et al. (2021); 2: Tan et al. (2019); 3: Li et al. (2018); 4: Liu et al. (2019); 5: Zhang et al. (2021); 6: Oswald et al. (2013); 7: Liu et al. (2020a); 8: Liu et al. (2020b); 9: Stutz et al. (2002); 10: Harrison and Kitto (1994); 11: Harrison et al. (1996); 12: Spindler et al. (1999); 13: Dillon et al. (2002); 14: Lin et al. (1996); 15: Kalthoff et al. (2000); 16: El Zein et al. (2013); 17: El Zein and Bedjanian (2012); 18: Romanias et al. (2012).

References

Cui, L., Li, R., Zhang, Y., Meng, Y., Fu, H., and Chen, J.: An observational study of nitrous acid (HONO) in Shanghai, China: The aerosol impact on HONO formation during the haze episodes, Science of The Total Environment, 630, 1057-1070, https://doi.org/10.1016/j.scitotenv.2018.02.063, 2018.

5 Dillon, M. B., Lamanna, M. S., Schade, G. W., Goldstein, A. H., and Cohen, R. C.: Chemical evolution of the Sacramento urban plume: Transport and oxidation, Journal of Geophysical Research: Atmospheres, 107, ACH 3-1-ACH 3-15, https://doi.org/10.1029/2001JD000969, 2002.

El Zein, A., and Bedjanian, Y.: Reactive Uptake of HONO to TiO2 Surface: "Dark" Reaction, The Journal of Physical Chemistry A, 116, 3665-3672, https://doi.org/10.1021/jp300859w, 2012.

10 El Zein, A., Romanias, M. N., and Bedjanian, Y.: Kinetics and Products of Heterogeneous Reaction of HONO with Fe2O3 and Arizona Test Dust, Environmental Science & Technology, 47, 6325-6331, https://doi.org/10.1021/es400794c, 2013.

Hao, Q., Jiang, N., Zhang, R., Yang, L., and Li, S.: Characteristics, sources, and reactions of nitrous acid during winter at an urban site in the Central Plains Economic Region in China, Atmos. Chem. Phys., 20,
15 7087-7102, https://doi.org/10.5194/acp-20-7087-2020, 2020.

Harrison, R. M., and Kitto, A.-M. N.: Evidence for a surface source of atmospheric nitrous acid, Atmospheric Environment, 28, 1089-1094, https://doi.org/10.1016/1352-2310(94)90286-0, 1994.

Harrison, R. M., Peak, J. D., and Collins, G. M.: Tropospheric cycle of nitrous acid, Journal of Geophysical Research: Atmospheres, 101, 14429-14439, https://doi.org/10.1029/96JD00341, 1996.

20 Heland, J., Kleffmann, J., Kurtenbach, R., and Wiesen, P.: A New Instrument To Measure Gaseous Nitrous Acid (HONO) in the Atmosphere, Environmental Science & Technology, 35, 3207-3212, https://doi.org/10.1021/es000303t, 2001.

Huang, Z., Zhong, Z., Sha, Q., Xu, Y., Zhang, Z., Wu, L., Wang, Y., Zhang, L., Cui, X., Tang, M., Shi, B., Zheng, C., Li, Z., Hu, M., Bi, L., Zheng, J., and Yan, M.: An updated model-ready emission inventory for
25 Guangdong Province by incorporating big data and mapping onto multiple chemical mechanisms, Science of The Total Environment, 769, 144535, https://doi.org/10.1016/j.scitotenv.2020.144535, 2021.

Jia, C., Tong, S., Zhang, W., Zhang, X., Li, W., Wang, Z., Wang, L., Liu, Z., Hu, B., Zhao, P., and Ge, M.: Pollution characteristics and potential sources of nitrous acid (HONO) in early autumn 2018 of Beijing, Science of The Total Environment, 735, 139317, https://doi.org/10.1016/j.scitotenv.2020.139317, 2020.

30 Kalthoff, N., Horlacher, V., Corsmeier, U., Volz-Thomas, A., Kolahgar, B., Geiß, H., Möllmann-Coers, M., and Knaps, A.: Influence of valley winds on transport and dispersion of airborne pollutants in the Freiburg-Schauinsland area, Journal of Geophysical Research: Atmospheres, 105, 1585-1597, https://doi.org/10.1029/1999JD900999, 2000.

Li, D., Xue, L., Wen, L., Wang, X., Chen, T., Mellouki, A., Chen, J., and Wang, W.: Characteristics and
35 sources of nitrous acid in an urban atmosphere of northern China: Results from 1-yr continuous observations, Atmospheric Environment, 182, 296-306, https://doi.org/10.1016/j.atmosenv.2018.03.033, 2018.

Lin, X., Roussel, P. B., Laszlo, S., Taylor, R., Meld, O. T., Shepson, P. B., Hastie, D. R., and Niki, H.: Impact of Toronto urban emissions on ozone levels downwind, Atmospheric Environment, 30, 2177-2193, https://doi.org/10.1016/1352-2310(95)00130-1, 1996.

Liu, J., Liu, Z., Ma, Z., Yang, S., Yao, D., Zhao, S., Hu, B., Tang, G., Sun, J., Cheng, M., Xu, Z., and Wang, Y.: Detailed budget analysis of HONO in Beijing, China: Implication on atmosphere oxidation capacity in polluted megacity, Atmospheric Environment, 244, 117957, https://doi.org/10.1016/j.atmosenv.2020.117957, 2021.

Liu, Y., Lu, K., Li, X., Dong, H., Tan, Z., Wang, H., Zou, Q., Wu, Y., Zeng, L., Hu, M., Min, K. E., Kecorius, S., Wiedensohler, A., and Zhang, Y.: A Comprehensive Model Test of the HONO Sources Constrained to Field Measurements at Rural North China Plain, Environ Sci Technol, https://doi.org/10.1021/acs.est.8b06367, 2019.

Liu, Y., Ni, S., Jiang, T., Xing, S., Zhang, Y., Bao, X., Feng, Z., Fan, X., Zhang, L., and Feng, H.: Influence of Chinese New Year overlapping COVID-19 lockdown on HONO sources in Shijiazhuang, Science of The Total Environment, 745, 141025, https://doi.org/10.1016/j.scitotenv.2020.141025, 2020a.

Liu, Y., Zhang, Y., Lian, C., Yan, C., Feng, Z., Zheng, F., Fan, X., Chen, Y., Wang, W., Chu, B., Wang, Y., Cai, J., Du, W., Daellenbach, K. R., Kangasluoma, J., Bianchi, F., Kujansuu, J., Petäjä, T., Wang, X., Hu, B., Wang, Y., Ge, M., He, H., and Kulmala, M.: The promotion effect of nitrous acid on aerosol formation in wintertime in Beijing: the possible contribution of traffic-related emissions, Atmos. Chem. Phys., 20, 13023-13040, https://doi.org/10.5194/acp-20-13023-2020, 2020b.

Meng, F., Qin, M., Tang, K., Duan, J., Fang, W., Liang, S., Ye, K., Xie, P., Sun, Y., Xie, C., Ye, C., Fu, P., Liu, J., and Liu, W.: High-resolution vertical distribution and sources of HONO and NO_2 in the nocturnal boundary layer in urban Beijing, China, Atmos. Chem. Phys., 20, 5071-5092, https://doi.org/10.5194/acp-20-5071-2020, 2020.

Oswald, R., Behrendt, T., Ermel, M., Wu, D., Su, H., Cheng, Y., Breuninger, C., Moravek, A., Mougin, E., Delon, C., Loubet, B., Pommerening-Röser, A., Sörgel, M., Pöschl, U., Hoffmann, T., Andreae, M. O., Meixner, F. X., and Trebs, I.: HONO Emissions from Soil Bacteria as a Major Source of Atmospheric Reactive Nitrogen, Science, 341, 1233-1235, https://doi.org/10.1126/science.1242266, 2013.

Romanias, M. N., El Zein, A., and Bedjanian, Y.: Reactive uptake of HONO on aluminium oxide surface, Journal of Photochemistry and Photobiology A: Chemistry, 250, 50-57, https://doi.org/10.1016/j.jphotochem.2012.09.018, 2012.

Shi, X., Ge, Y., Zheng, J., Ma, Y., Ren, X., and Zhang, Y.: Budget of nitrous acid and its impacts on atmospheric oxidative capacity at an urban site in the central Yangtze River Delta region of China, Atmospheric Environment, 238, 117725, https://doi.org/10.1016/j.atmosenv.2020.117725, 2020.

Spataro, F., Ianniello, A., Esposito, G., Allegrini, I., Zhu, T., and Hu, M.: Occurrence of atmospheric nitrous acid in the urban area of Beijing (China), Science of The Total Environment, 447, 210-224, https://doi.org/10.1016/j.scitotenv.2012.12.065, 2013.

Spindler, G., Brüggemann, E., and Herrmann, H.: Nitrous acid (HNO_2) concentration measurements and estimation of dry deposition over grassland in eastern Germany, Proceedings of the EUROTRAC Symposium 1998, Vol. 2, WITpress, Southampton, UK, 218–222, 1999.

Stutz, J., Alicke, B., and Neftel, A.: Nitrous acid formation in the urban atmosphere: Gradient measurements of NO_2 and HONO over grass in Milan, Italy, Journal of Geophysical Research: Atmospheres, 107, 8192, https://doi.org/10.1029/2001JD000390, 2002.

80   Stutz, J., Alicke, B., Ackermann, R., Geyer, A., Wang, S., White, A. B., Williams, E. J., Spicer, C. W., and Fast, J. D.: Relative humidity dependence of HONO chemistry in urban areas, Journal of Geophysical Research: Atmospheres, 109, https://doi.org/10.1029/2003JD004135, 2004.

Tan, Z., Lu, K., Hofzumahaus, A., Fuchs, H., Bohn, B., Holland, F., Liu, Y., Rohrer, F., Shao, M., Sun, K., Wu, Y., Zeng, L., Zhang, Y., Zou, Q., Kiendler-Scharr, A., Wahner, A., and Zhang, Y.: Experimental
85   budgets of OH, HO2, and RO2 radicals and implications for ozone formation in the Pearl River Delta in China 2014, Atmos. Chem. Phys., 19, 7129-7150, https://doi.org/10.5194/acp-19-7129-2019, 2019.

Tian, Z., Yang, W., Yu, X., Zhang, M., Zhang, H., Cheng, D., Cheng, P., and Wang, B.: HONO pollution characteristics and nighttime sources during autumn in Guangzhou, China Environmental Science, 39 (05), 2000-2009, https://doi.org/10.13227/j.hjkx.201709269, 2018.

90   Tong, S., Hou, S., Zhang, Y., Chu, B., Liu, Y., He, H., Zhao, P., and Ge, M.: Comparisons of measured nitrous acid (HONO) concentrations in a pollution period at urban and suburban Beijing, in autumn of 2014, Science China Chemistry, 58, 1393-1402, https://doi.org/10.1007/s11426-015-5454-2, 2015.

Tong, S., Hou, S., Zhang, Y., Chu, B., Liu, Y., He, H., Zhao, P., and Ge, M.: Exploring the nitrous acid (HONO) formation mechanism in winter Beijing: direct emissions and heterogeneous production in urban
95   and suburban areas, Faraday Discuss, 189, 213-230, https://doi.org/10.1039/C5FD00163C, 2016.

Trebs, I., Meixner, F. X., Slanina, J., Otjes, R., Jongejan, P., and Andreae, M. O.: Real-time measurements of ammonia, acidic trace gases and water-soluble inorganic aerosol species at a rural site in the Amazon Basin, Atmos. Chem. Phys., 4, 967-987, https://doi.org/10.5194/acp-4-967-2004, 2004.

Villena, G., Bejan, I., Kurtenbach, R., Wiesen, P., and Kleffmann, J.: Development of a new Long Path
100   Absorption Photometer (LOPAP) instrument for the sensitive detection of NO_2 in the atmosphere, Atmos. Meas. Tech., 4, 1663-1676, https://doi.org/10.5194/amt-4-1663-2011, 2011.

Wang, B. G., Zhu, D., Zou, Y., Wang, H., Zhou, L., Ouyang, X., Shao, H. F., and Deng, X. J.: Source analysis of peroxyacetyl nitrate (PAN) in Guangzhou, China: a yearlong observation study, Atmos. Chem. Phys. Discuss., 2015, 17093-17133, https://doi.org/10.5194/acpd-15-17093-2015, 2015a.

105   Wang, L., Wen, L., Xu, C., Chen, J., Wang, X., Yang, L., Wang, W., Yang, X., Sui, X., Yao, L., and Zhang, Q.: HONO and its potential source particulate nitrite at an urban site in North China during the cold season, Science of The Total Environment, 538, 93-101, https://doi.org/10.1016/j.scitotenv.2015.08.032, 2015b.

Zhang, S., Sarwar, G., Xing, J., Chu, B., Xue, C., Sarav, A., Ding, D., Zheng, H., Mu, Y., Duan, F., Ma, T., and He, H.: Improving the representation of HONO chemistry in CMAQ and examining its impact on
110   haze over China, Atmos. Chem. Phys., 21, 15809-15826, https://doi.org/10.5194/acp-21-15809-2021, 2021.

Zhang, W., Tong, S., Ge, M., An, J., Shi, Z., Hou, S., Xia, K., Qu, Y., Zhang, H., Chu, B., Sun, Y., and He, H.: Variations and sources of nitrous acid (HONO) during a severe pollution episode in Beijing in winter 2016, Science of The Total Environment, 648, 253-262, https://doi.org/10.1016/j.scitotenv.2018.08.133,
115   2019.